STABILITY AND DYNAMICS OF QUANTIZED VORTICES IN GASEOUS BOSE-EINSTEIN CONDENSATES

Jukka Huhtamäki

Department of Engineering Physics
Helsinki University of Technology
Espoo, Finland

Dissertation for the degree of Doctor of Science in Technology to be presented with due permission of the Faculty of Information and Natural Sciences for public examination and debate in Auditorium D at Helsinki University of Technology (Espoo, Finland) on the 7th of March, 2008, at 13 o'clock.

Dissertations of Department of Engineering Physics
Helsinki University of Technology
ISSN 1455-1802

Dissertation 153 (2008):
Jukka Huhtamäki: Stability and dynamics of quantized vortices in gaseous Bose-Einstein condensates

Opponent:
Prof. Martin Holthaus, Carl von Ossietzky Universität, Germany

Pre-examiners:
Assist. Prof. Jani-Petri Martikainen, NORDITA, Sweden
Assist. Prof. Emil Lundh, Umeå University, Sweden

ISBN 978-951-22-9255-4 (print)
ISBN 978-951-22-9256-1 (electronic)

Multiprint Oy/Otamedia
Espoo 2008

ABSTRACT OF DOCTORAL DISSERTATION	HELSINKI UNIVERSITY OF TECHNOLOGY P. O. BOX 1000, FI-02015 TKK http://www.tkk.fi

Author Huhtamäki, Jukka Antti Mikael

Name of the dissertation

Stability and dynamics of quantized vortices in gaseous Bose-Einstein condensates

Manuscript submitted 11.12.2007	Manuscript revised
Date of the defence 7.3.2008	
☐ Monograph	☒ Article dissertation (summary + original articles)

Faculty	Faculty of Information and Natural Sciences
Department	Department of Engineering Physics
Field of research	Bose-Einstein condensation
Opponent(s)	Prof. Martin Holthaus
Supervisor	Acad. Prof. Risto Nieminen
Instructor	Dr. Sami Virtanen, Dr. Mikko Möttönen

Abstract

Bose-Einstein condensation is a quantum statistical phase transition which was theoretically predicted almost a hundred years ago. After years of seminal research, physicists realized the first almost ideal Bose-Einstein condensates in ultracold dilute atomic gases in 1995. Since then, the theoretical and experimental methods concerning such systems have been developing rapidly, and many fascinating phenomena have been found in these novel quantum systems.

Bose-Einstein condensation occurs in a system consisting of massive bosons when a single quantum state becomes macroscopically occupied as the temperature is lowered below the transition temperature. In general, condensates consisting of repulsively interacting bosons exhibit superfluidity: Particle currents can flow in the system without dissipation and viscosity. Moreover, the velocity fields of condensates have to be irrotational, which severely restricts the rotational characteristics of these systems. Apart from the center of mass motion, the system may carry angular momentum in the form of elementary excitations or so-called quantized vortices.

This Thesis is a theoretical study of subjects related to stability and dynamics of quantized vortices in dilute atomic Bose-Einstein condensates. The precession and instability of off-centered vortices in trapped condensates is investigated both in the zero-temperature limit and at finite temperatures. Dynamical stability of multiply quantized vortices and vortex clusters is studied in axisymmetric trap geometries. Splitting of energetically and dynamically unstable multiply quantized vortices into singly quantized vortices is also studied. Finally, as a separate subject, tunneling of a condensate through a potential barrier is investigated. Majority of this work relies on numerical methods for solving the Gross-Pitaevskii and Bogoliubov equations, which are of central importance in the study of dilute atomic Bose-Einstein condensates.

Keywords Bose-Einstein condensation, superfluidity, vortex

ISBN (printed) 978-951-22-9255-4	ISSN (printed) 1455-1802
ISBN (pdf) 978-951-22-9256-1	ISSN (pdf)
Language english	Number of pages 116

Publisher Department of Engineering Physics, Helsinki University of Technology

Print distribution

☒ The dissertation can be read at http://lib.tkk.fi/Diss/2008/isbn9789512292561/

VÄITÖSKIRJAN TIIVISTELMÄ	TEKNILLINEN KORKEAKOULU PL 1000, 02015 TKK http://www.tkk.fi

Tekijä Huhtamäki, Jukka Antti Mikael

Väitöskirjan nimi

Kvantittuneiden vorteksien stabiilisuus ja dynamiikka kaasumaisissa Bose-Einstein -kondensaateissa

Käsikirjoituksen päivämäärä 11.12.2007	Korjatun käsikirjoituksen päivämäärä
Väitöstilaisuuden ajankohta 7.3.2008	
☐ Monografia	☒ Yhdistelmäväitöskirja (yhteenveto + erillisartikkelit)

Tiedekunta	Informaatio- ja luonnontieteiden tiedekunta
Laitos	Teknillisen fysiikan laitos
Tutkimusala	Bose-Einstein -kondensaatio
Vastaväittäjä(t)	prof. Martin Holthaus
Työn valvoja	akat. prof. Risto Nieminen
Työn ohjaaja	TkT Sami Virtanen, TkT Mikko Möttönen

Tiivistelmä

Bose-Einstein -kondensaatio on kvanttistatistinen faasitransitio, jonka olemassaolo ennustettiin teoreettisesti jo lähes sata vuotta sitten. Vuosien urauuurtavan tutkimustyön tuloksena vuonna 1995 onnistuttiin realisoimaan kokeellisesti ensimmäiset lähes ideaaliset Bose-Einstein -kondensaatit erittäin kylmissä atomikaasuissa. Tämän jälkeen aiheeseen liittyvät teoreettiset ja kokeelliset menetelmät ovat kehittyneet nopeasti ja monia mielenkiintoisia ilmiöitä on löydetty näistä uudenlaisista kvanttimekaanisista systeemeistä.

Bose-Einstein -kondensaatio tapahtuu massallisista bosoneista koostuvissa systeemeissä kun yksi kvanttitila miehittyy makroskooppisesti lämpötilan alittaessa transitiolämpötilan. Repulsiivisesti vuorovaikuttavista hiukkasista koostuva kondensaatti on yleensä on suprajuokseva: Hiukkaset voivat virrata systeemissä ilman kitkaa tai viskositeettia. Tämän lisäksi kondensaatin nopeuskentän on oltava pyörteetön, mikä rajoittaa systeemin pyörimistä: massakeskipisteliikkeen lisäksi kondensaatti voi sisältää kulmaliikemäärää eksitaatioina ja niin sanottuina kvantittuneina vortekseina.

Tässä väitöskirjassa tarkastellaan teoreettisesta näkökulmasta aiheita, jotka liittyvät kvantittuneiden vorteksien stabiilisuuteen ja dynamiikkaan heikosti vuorovaikuttavissa Bose-Einstein -kondensaateissa. Epäkeskisten vorteksien prekessiota ja epästabiilisuutta tutkitaan loukutetuissa kondensaateissa sekä nollalämpötilan rajalla että äärellisissä lämpötiloissa. Monikvanttivorteksien ja vorteksiklustereiden dynaamista stabiilisuutta tarkastellaan sylinterisymmetrisissä loukuissa. Lisäksi tutkitaan energeettisesti ja dynaamisesti epästabiilien monikvanttivorteksien jakautumista yksikvanttivortekseiksi. Lopuksi tarkastellaan erillisenä aiheena kondensaatin tunneloitumista potentiaalivallin lävitse. Suuri osa työstä pohjautuu Gross-Pitaevskii ja Bogoliubov -yhtälöiden numeeriseen ratkaisemiseen. Nämä yhtälöt ovat keskeisessä roolissa harvoista atomikaasuista koostuvien Bose-Einstein -kondensaattien mallintamisessa.

Asiasanat Bose-Einstein -kondensaatio, suprajuoksevuus, vorteksi

ISBN (painettu) 978-951-22-9255-4	ISSN (painettu) 1455-1802
ISBN (pdf) 978-951-22-9256-1	ISSN (pdf)
Kieli englanti	Sivumäärä 116

Julkaisija Teknillisen fysiikan laitos, Teknillinen korkeakoulu

Painetun väitöskirjan jakelu

☒ Luettavissa verkossa osoitteessa http://lib.tkk.fi/Diss/2008/isbn9789512292561/

Affiliation

Author

Jukka Huhtamäki

Laboratory of Physics

Helsinki University of Technology

Espoo, Finland

Supervisor

Acad. Prof. Risto Nieminen

Laboratory of Physics

Helsinki University of Technology

Espoo, Finland

Opponent

Prof. Martin Holthaus

Institut für Physik

Carl von Ossietzky Universität

Oldenburg, Germany

Reviewer

Assist. Prof. Jani-Petri Martikainen

Nordic Institute for Theoretical Physics

University of Stockholm

Stockholm, Sweden

Reviewer

Assist. Prof. Emil Lundh

Department of Physics

Umeå University

Umeå, Sweden

Preface

The research reviewed in this Thesis started in the year 2002 in the Materials Physics Laboratory, Helsinki University of Technology, where I was working as an undergraduate student. After completing my Master's Thesis in 2004 on quantum optics, I continued research in the field of Bose-Einstein condensates as a graduate student. Research during the years 2005-2007 has been carried out in the Laboratory of Physics.

For financial support, I would like to thank the Finnish Cultural Foundation, the Vilho, Yrjö and Kalle Väisälä foundation, and the Magnus Ehrnrooth Foundation. CSC, the Finnish IT center for science, is acknowledged for computational resources.

I would like to thank my supervisors Prof. M. M. Salomaa and Acad. Prof. R. M. Nieminen for providing excellent working facilities, as well as our group leader Dr. A. Harju for keeping the computers running. I am grateful to my instructors Dr. T. Isoshima, Dr. M. Möttönen, and, in particular, my mentor Dr. S. Virtanen, who had the patience to answer every single one of my questions and taught me so much else than just physics. M.Sc. V. Pietilä and other collaborators are acknowledged for fruitful scientific cooperation. Dr. Y. Shin is acknowledged for providing Fig. 4.1.

I would also like to thank my brothers, Markus and Henri, and my parents, Vuokko and Seppo, for support and the best family to grow up in. I am grateful to my relatives, H. Sevä and all of my other friends, and my girlfriend Miia for making my spare time delightful.

Espoo, December 2007

Jukka Huhtamäki

Contents

List of Publications

I Tomoya Isoshima, Jukka Huhtamäki, and Martti M. Salomaa, *Instabilities of off-centered vortices in a Bose-Einstein condensate*, Phys. Rev. A **68**, 033611 (2003).

II Tomoya Isoshima, Jukka Huhtamäki, and Martti M. Salomaa, *Precessional motion of a vortex in a finite-temperature Bose-Einstein condensate*, Phys. Rev. A **69**, 063601 (2004).

III J. A. M. Huhtamäki, M. Möttönen, and S. M. M. Virtanen, *Dynamically stable multiply quantized vortices in dilute Bose-Einstein condensates*, Phys. Rev. A **74**, 063619 (2006).

IV V. Pietilä, M. Möttönen, T. Isoshima, J. A. M. Huhtamäki, and S. M. M. Virtanen, *Stability and dynamics of vortex clusters in nonrotated Bose-Einstein condensates*, Phys. Rev. A **74**, 023603 (2006).

V J. A. M. Huhtamäki, M. Möttönen, T. Isoshima, V. Pietilä, and S. M. M. Virtanen, *Splitting Times of Doubly Quantized Vortices in Dilute Bose-Einstein Condensates*, Phys. Rev. Lett. **97**, 110406 (2006).

VI T. Isoshima, M. Okano, H. Yasuda, K. Kasa, J. A. M. Huhtamäki, M. Kumakura, and Y. Takahashi, *Spontaneous Splitting of a Quadruply Charged Vortex*, Phys. Rev. Lett. **99**, 200403 (2007).

VII J. A. M. Huhtamäki, M. Möttönen, J. Ankerhold, and S. M. M. Virtanen, *Effects of interactions and noise on tunneling of Bose-Einstein condensates through a potential barrier*, Phys. Rev. A **76**, 033605 (2007).

Author's contribution

The research presented in this Thesis was carried out in the Materials Physics Laboratory as an undergraduate student during 2002-2004 and as a graduate student during 2004-2005, and in the Laboratory of Physics during 2005-2007.

In Papers I–II, the author was actively involved with the numerical simulations concerning the research. Paper III was mostly written by the author, and all numerical calculations were performed by him. The author participated in finishing the manuscript of Paper IV. In Paper V, the author was the principal writer, and all numerical and analytical calculations were carried out by him. The author contributed to the research work presented in Paper VI by performing simulations and participating in writing the manuscript. Paper VII was written by the author, and all numerical and analytical calculations were performed by him. Additionally, the author has given several presentations concerning the reseach in domestic and international conferences.

1 Introduction

The theoretical prediction of a quantum statistical phase transition in a system of massive bosons dates back to 1924-1925 when A. Einstein published the quantum theory of an ideal bose gas [1, 2] based on S. N. Bose's recent statistical derivation of Planck's radiation law [3]. In his work, Einstein concluded that in a gas of non-interacting massive bosons, a significant fraction of the particles will occupy the lowest-lying single-particle state below a critical temperature. This phenomenon, later known as Bose-Einstein condensation, occurs also in certain interacting gases as well as in strongly interacting systems. Later on, it has been related to such fundamental concepts as superconductivity, discovered by H. Kamerlingh-Onnes in 1911 [4], and superfluidity of ^{4}He discovered by P. L. Kapitza, F. J. Allen, and A. D. Misener [5, 6]. However, in such a strongly interacting system, the relation to Bose-Einstein condensation (BEC) is not obvious because only a fraction of the particles reside in the lowest-lying single-particle state even in the zero-temperature limit.

Nearly ideal Bose-Einstein condensation was finally realized experimentally in 1995 using trapped vapours of ^{87}Rb [7], ^{23}Na [8], and ^{7}Li [9] which has effectively attractive atom-atom interactions. Condensation in dilute atomic gases is quite exceptional: due to the weak interactions between the atoms, the fraction of particles in the condensate is relatively large, well exceeding $\frac{1}{2}$ already in the early experiments [9, 10]. The weakly-interacting system can be modeled using a simple mean-field approach, which is inapplicable to systems with strong interactions because of significant correlation effects. Due to the diluteness of the gas, the natural length scales in the system are relatively large, providing the possibility to measure directly optically, for example, the density profiles of these systems yielding direct information on relevant physical quantities. Furthermore, the diluteness of the gas greatly suppresses the three-body recombination events which are responsible for the formation of molecules, and thus increases the lifetime of the condensate [11]. As opposed to, *e.g.*, helium superfluids, the inhomogeneity of trapped gases allows the observation of condensation not only in momentum, but also in real space.

Neutral alkali atoms are well suited for magnetic and optical trapping. Majority of condensates evoked to date consist of alkali atoms due to their advantageous internal structure for laser cooling. All stable alkali species have been condensed: In addition to the aforementioned gases, BEC has been achieved also in ^{41}K [12], ^{39}K [13], ^{85}Rb [14], and ^{133}Cs [15]. Besides alkali gases, BEC has been realized also using vapours of spin-polarized H [16], metastable ^{4}He [17], ^{174}Yb [18], ^{6}Li$_2$ molecules [19], ^{40}K$_2$ molecules [20], and ^{52}Cr [21] which has a relatively large magnetic dipole moment compared to the other atom species. Several Feshbach resonances have been found in many of these gases, which turn out to be extremely convenient for controlling the effective atom-atom interaction strength in purely optical traps by using magnetic bias fields.

In a typical experiment, the number of atoms in the dilute Bose-Einstein condensate is of the order of 10^6, the dimensions of the cloud is of the order of 10-100 μm, yielding roughly a particle density of 10^{14} atoms/cm^3. The critical temperature for the occurrence of condensation is of the order of $T_{\mathrm{BEC}} = 1\ \mu$K.

A Bose-Einstein condensate can be accurately described by a macroscopic wave function, also known as the order parameter. The amplitude of this complex-valued function is directly related to the density of the condensed particles and its phase gradient to the average particle velocity. The elementary excitation spectrum of a weakly-interacting Bose gas, which determines the density fluctuations in the system, was derived in 1947 by Bogoliubov in an attempt of explaining the phenomenon of superfluidity in helium II [22]. The low-energy excitations are phonons, *i.e.*, collective modes with an approximately linear dispersion relation in the thermodynamic limit, and the high-energy excitations are essentially single-particle modes with a quadratic dispersion relation [23]. The eigenfrequencies of the energetically lowest-lying collective modes of a harmonically confined condensate have been theoretically predicted to deviate from the ideal gas case, and the frequencies were demonstrated to depend on the effective interaction strength between the atoms [24–28]. The experimentally measured frequencies [29–31] are in very good agreement with the theoretical results.

One of the key signatures of Bose-Einstein condensation is superfluidity. In superfluids, particle currents may flow without viscosity and dissipation. This phenomenon is typically a consequence of the existence of a macroscopic wave function which manifests the phase coherence among the condensed particles. Direct evidence of superfluidity has been obtained by measuring the frequencies of the so-called scissors modes of Bose-Einstein condensates [32–34]. Furthermore, the velocity field in a condensate has to be irrotational, resulting in a reduced moment of inertia [35–37] which is typical for superfluids. This reduction has been verified experimentally by observing the expansion of a rotating condensate [38]. The Landau critical velocity for the onset of dissipative flow has been measured by moving a laser beam through a condensate [39].

The requirement of irrotationality of the condensate velocity field gives rise to quantized vorticity in the system, which was first observed experimentally by Matthews *et al.* [40]. The quantized vortex is an example of a state with a persistent nonviscous particle flow. In addition to dilute atomic Bose-Einstein condensates, vortices play an essential role in liquid helium [41,42] and superconductors [43], and they have been observed also in coherent optical fields [44]. The 2π winding of the complex phase around the vortex core has been measured using so-called phase contrast imaging [40, 45], demonstrating that the vortex state contains angular momentum. The presence of a vortex shifts the eigenfrequencies of the quadrupole modes of the condensate [46] resulting in rotational motion of the system. By exploiting this effect, the angular momentum of a condensate containing one or more vortices created by stirring the system with a laser beam has been measured [47].

This Thesis is a theoretical study of the stability and dynamics of vortices in dilute atomic Bose-Einstein condensates. The theoretical formalism required for understanding the concepts in the subsequent sections and the publications is outlined in Section 2. In particular, the mean-field formalism is introduced, and the Gross-Pitaevskii and the Bogoliubov equations are derived, which are of central importance in the publications included in this Thesis. In Section 3, theoretical aspects concerning vortices in Bose-Einstein condensates are briefly reviewed with emphasis on the energetic and dynamic stability of the vortex states. Also, the main results of Papers I–IV are discussed. Section 4 concerns experiments with quantized vortices in Bose-Einstein condensates. The methods used for creating the first singly quantized vortices, vortex lattices, and multiply quantized vortices are briefly explained and their successful implementations are discussed. The splitting times of doubly quantized vortices obtained from simulations described in Paper V are compared with the results of the closely related experiments. Also, the splitting of a quadruply quantized vortex, which is the topic of Paper VI, is discussed. Before the final conclusions, dynamics of Bose-Einstein condensates in optical lattices is discussed in Section 5. This subject is closely related to the tunneling of a Bose-Einstein condensate through a potential barrier investigated in Paper VII.

2 Mean-Field Theory of Dilute Bose-Einstein Condensates

This Thesis concerns mostly single-component (scalar) condensates, in which the hyperfine spin degree of freedom is frozen to a single quantum state, *e.g.*, due to an external magnetic field. Hence, we will discuss the mean field theory only in the scalar case. Generalization to the multi-component case is quite straightforward [48–50].

2.1 Definition of Bose-Einstein Condensation

The system under study consists of N identical interacting bosons in a fixed spin state, confined by some external potential. Due to the bosonic nature of the particles, the many-body wave function $\Psi(\mathbf{r}_1, \mathbf{r}_2, \ldots, \mathbf{r}_N; t)$, where $\mathbf{r}_i$ denote the particle coordinates, of the system must be symmetric with respect to interchange of particle indices. The one-body density matrix $\rho(\mathbf{r}, \mathbf{r}'; t)$ of the system, occupying the orthonormal states $\Psi_N^{(s)}$ with probabilities p_s, is given by [50]

$$\rho(\mathbf{r}, \mathbf{r}'; t) = N \sum_s p_s \int d\mathbf{r}_2 \ldots d\mathbf{r}_N \left[\Psi_N^{(s)}(\mathbf{r}, \mathbf{r}_2, \ldots, \mathbf{r}_N; t)\right]^* \Psi_N^{(s)}(\mathbf{r}', \mathbf{r}_2, \ldots, \mathbf{r}_N; t). \quad (2.1)$$

The diagonal part of the density matrix yields the density of particles, whereas the non-diagonal elements reveal the long-range order possibly present in the system. Clearly, the matrix function $\rho(\mathbf{r}, \mathbf{r}'; t)$ is Hermitian, and hence it can be diagonalized in terms of single-particle eigenfunctions $\varphi_\alpha(\mathbf{r}, t)$ as

$$\rho(\mathbf{r}, \mathbf{r}'; t) = \sum_\alpha N_\alpha(t) \varphi_\alpha^*(\mathbf{r}, t) \varphi_\alpha(\mathbf{r}', t), \quad (2.2)$$

where the eigenvalues $N_\alpha(t)$ are real. (Simple) Bose-Einstein condensation takes place if there exists exactly one eigenvalue which is of the order of the total number of particles, $N_0 \sim N$, and the rest of the eigenvalues are much smaller $N_{\alpha\neq 0} \ll N_0$. The single-particle wave function $\varphi_0(\mathbf{r}, t)$ corresponding to the macroscopic eigenvalue is referred to as the order parameter, or the macroscopic wave function, of the condensate.

2.2 The Bogoliubov Approximation

The bosonic field operator $\hat{\psi}(\mathbf{r}, t)$ in the Heisenberg picture can be written in terms of the single-particle wave functions $\varphi_\alpha(\mathbf{r}, t)$ and the corresponding bosonic creation and annihilation operators[1], $\hat{a}_\alpha^\dagger$ and $\hat{a}_\alpha$, as

$$\hat{\psi}(\mathbf{r}, t) = \sum_\alpha \varphi_\alpha(\mathbf{r}, t)\hat{a}_\alpha, \tag{2.3}$$

where the bosonic creation and annihilation operators obey the usual equal-time canonical commutation relations

$$[\hat{a}_\alpha, \hat{a}_\beta^\dagger] = \delta_{\alpha\beta}, \qquad [\hat{a}_\alpha, \hat{a}_\beta] = 0, \qquad [\hat{a}_\alpha^\dagger, \hat{a}_\beta^\dagger] = 0, \tag{2.4}$$

and the single-particle wave functions are assumed to be orthonormal

$$\int d\mathbf{r}\, \varphi_\alpha^*(\mathbf{r}, t)\varphi_\beta(\mathbf{r}, t) = \delta_{\alpha\beta}. \tag{2.5}$$

It is natural to split the sum in Eq. (2.3) into two parts

$$\hat{\psi}(\mathbf{r}, t) = \varphi_0(\mathbf{r}, t)\hat{a}_0 + \sum_{\alpha\neq 0} \varphi_\alpha(\mathbf{r}, t)\hat{a}_\alpha. \tag{2.6}$$

In the Bogoliubov approximation the operator $\hat{a}_0$, corresponding to the condensate state, is substituted with the real number $\sqrt{N_0}$, which amounts to neglecting the noncommutativity of the operator [22]. Hence, the field operator is given as a sum of a classical field $\Psi = \sqrt{N_0}\varphi_0$ (condensate) and an operator accounting for the quantum and thermal fluctuations $\hat{\phi} = \sum_{\alpha\neq 0} \varphi_\alpha \hat{a}_\alpha$ (noncondensate) as

$$\hat{\psi}(\mathbf{r}, t) = \Psi(\mathbf{r}, t) + \hat{\phi}(\mathbf{r}, t), \tag{2.7}$$

where the noncondensate part is assumed to be a small correction to the condensate wave function [51]. The condensate wave function is given by the ground-state expectation value of the field operator, $\Psi(\mathbf{r}, t) = \langle\hat{\psi}(\mathbf{r}, t)\rangle$.

---

[1] In fact, the operators $\hat{a}_\alpha^{(\dagger)}$ are also in the Heisenberg picture, but for simplicity we will not state their time dependence explicitly.

2.3 The Gross-Pitaevskii Equation in the Low Temperature Limit

The effective grand-canonical Hamiltonian for the dilute Bose gas in a frame rotating with the angular frequency $\mathbf{\Omega}$ has the form

$$\hat{K_\Omega} = \hat{H_\Omega} - \mu\hat{N} = \int d\mathbf{r}\,\hat{\psi}^\dagger\left[\hat{h}_\Omega - \mu\right]\hat{\psi} + \frac{g}{2}\int d\mathbf{r}\,\hat{\psi}^\dagger\hat{\psi}^\dagger\hat{\psi}\hat{\psi}, \tag{2.8}$$

where μ is the chemical potential and $\hat{N}$ is the particle number operator. Above, the two-body interaction potential has been replaced by a delta function, $\hat{V}(\mathbf{r}-\mathbf{r}') = g\delta(\mathbf{r}-\mathbf{r}')$, yielding the same scattering properties at low energies as the actual potential. $\hat{h}_\Omega = -\frac{\hbar^2}{2m}\nabla^2 + V_{\text{ext}}(\mathbf{r},t) - \mathbf{\Omega}\cdot\hat{L}$ is the Hamiltonian of a single particle in the external potential V_{ext} in a rotating frame [52] with $\hat{L}$ being the angular momentum operator. The coupling constant is related to the s-wave scattering length a by $g = 4\pi\hbar^2 a/m$, where m is the particle mass [53]. The field operator must satisfy the Heisenberg equation of motion[2]

$$i\hbar\frac{\partial}{\partial t}\hat{\psi} = [\hat{\psi}, \hat{K}_\Omega] = \left[\hat{h}_\Omega - \mu + g\hat{\psi}^\dagger\hat{\psi}\right]\hat{\psi}. \tag{2.9}$$

In the low temperature limit, $T \ll T_{BEC}$, and for low enough densities, the non-condensate component $\hat{\phi}$ may be neglected to a good approximation, and hence by substituting $\hat{\psi} \to \Psi$, we obtain the time-dependent Gross-Pitaevskii equation

$$i\hbar\frac{\partial}{\partial t}\Psi(\mathbf{r},t) = \left[\hat{h}_\Omega - \mu + g|\Psi(\mathbf{r},t)|^2\right]\Psi(\mathbf{r},t), \tag{2.10}$$

which is used extensively in Papers I and IV–VII for solving the time evolution of the condensate. For a time-independent external potential $V_{\text{ext}}(\mathbf{r})$, stationary states are solutions to the time-independent Gross-Pitaevskii equation

$$\left[\hat{h}_\Omega - \mu + g|\Psi(\mathbf{r})|^2\right]\Psi(\mathbf{r}) = 0, \tag{2.11}$$

which play a central role in Papers III and IV.

A simple approximation for the ground state of the condensate in a non-rotating frame is obtained by neglecting the kinetic energy term in Eq. (2.11), yielding

$$\Psi_{\text{TF}}(\mathbf{r}) = \sqrt{\frac{\mu - V_{\text{ext}}(\mathbf{r})}{g}}, \tag{2.12}$$

[2]Naturally, the field operator is time independent in the Schödinger picture.

for $V_{\text{ext}}(\mathbf{r}) < \mu$, and zero otherwise. This is called the Thomas-Fermi (TF) approximation for the wave function. The approximation is accurate in the interior of the condensate when the parameter Na is much larger than the typical length scale of the external potential [23]. This requirement is often satisfied in experimental configurations and it is one of the key approximations used for calculating the tunneling rate of a condensate through a potential barrier in Paper VII.

2.4 Elementary Excitations in the Low Temperature Limit

In this section, we will study the low-energy collective oscillations of the condensate in the ultralow temperature limit, such that the order parameter satisfies Eq. (2.11). The Hamiltonian in Eq. (2.8) is treated in a mean-field approximation and diagonalized by a canonical transformation.

Small-amplitude oscillations around a given stationary state $\Psi(\mathbf{r})$ can be studied by writing the field operator in the form [51], *c.f.* Sec. 2.2,

$$\hat{\psi}(\mathbf{r}, t) = \Psi(\mathbf{r}) + \hat{\phi}(\mathbf{r}, t). \tag{2.13}$$

By substituting this form into the Heisenberg equation of motion for the field operator, Eq. (2.9), and neglecting terms higher than linear order in $\hat{\phi}$, we obtain an equation of motion for the fluctuation operator

$$i\hbar \frac{\partial}{\partial t} \hat{\phi}(\mathbf{r}, t) = \mathcal{L}(\mathbf{r})\hat{\phi}(\mathbf{r}, t) + \mathcal{M}(\mathbf{r})\hat{\phi}^\dagger(\mathbf{r}, t), \tag{2.14}$$

where $\mathcal{L}(\mathbf{r}) = \hat{h}_\Omega - \mu + 2g|\Psi(\mathbf{r})|^2$ and $\mathcal{M}(\mathbf{r}) = g[\Psi(\mathbf{r})]^2$.

Bogoliubov Transformation and the Bogoliubov Equations

In order to solve Eq. (2.14), we introduce the quasiparticle creation and annihilation operators $\hat{b}_\alpha^\dagger$ and $\hat{b}_\alpha$, respectively, related to the original creation and annihilation operators through [54]

$$\hat{b}_\alpha^\dagger = \sum_{\beta \neq 0} U_{\alpha\beta} \hat{a}_\beta^\dagger - V_{\alpha\beta} \hat{a}_\beta, \tag{2.15}$$

$$\hat{b}_\alpha = \sum_{\beta \neq 0} U_{\alpha\beta}^* \hat{a}_\beta - V_{\alpha\beta}^* \hat{a}_\beta^\dagger. \tag{2.16}$$

In order for the transformation to be canonical, the coefficient matrices U and V are required to satisfy

$$UU^\dagger - VV^\dagger = I, \qquad UV^T - VU^T = 0, \tag{2.17}$$

which imply the inverse transformation

$$\hat{a}^\dagger_\alpha = \sum_{\beta\neq 0} U^*_{\beta\alpha}\hat{b}^\dagger_\beta + V_{\beta\alpha}\hat{b}_\beta, \tag{2.18}$$

$$\hat{a}_\alpha = \sum_{\beta\neq 0} U_{\beta\alpha}\hat{b}_\beta + V^*_{\beta\alpha}\hat{b}^\dagger_\beta. \tag{2.19}$$

Hence, we may write the fluctuation operator in the form

$$\hat{\phi}(\mathbf{r},t) = \sum_{\alpha\neq 0}\varphi_\alpha(\mathbf{r},t)\hat{a}_\alpha = \sum_{\beta\neq 0} u_\beta(\mathbf{r},t)\hat{b}_\beta + v^*_\beta(\mathbf{r},t)\hat{b}^\dagger_\beta, \tag{2.20}$$

where

$$u_\beta(\mathbf{r},t) = \sum_{\alpha\neq 0} U_{\beta\alpha}\varphi_\alpha(\mathbf{r},t), \qquad v_\beta(\mathbf{r},t) = \sum_{\alpha\neq 0} V_{\beta\alpha}\varphi^*_\alpha(\mathbf{r},t), \tag{2.21}$$

are called the quasiparticle wave functions. By using the orthonormality of the single-particle wave functions $\varphi_\alpha(\mathbf{r},t)$ and Eqs. (2.17), we note that in order for the transformation to be canonical the following equations must be satisfied:

$$\int d\mathbf{r}\left[u_\alpha(\mathbf{r},t)u^*_\beta(\mathbf{r},t) - v_\alpha(\mathbf{r},t)v^*_\beta(\mathbf{r},t)\right] = \delta_{\alpha\beta}, \tag{2.22}$$

$$\int d\mathbf{r}\left[u_\alpha(\mathbf{r},t)v_\beta(\mathbf{r},t) - v_\alpha(\mathbf{r},t)u_\beta(\mathbf{r},t)\right] = 0, \tag{2.23}$$

where the first equation is the orthonormality condition for the quasiparticle wave functions. Expecting oscillatory solutions, we choose the time dependence of the quasiparticle wave functions according to

$$u_\alpha(\mathbf{r},t) = u_\alpha(\mathbf{r})e^{-i\omega_\alpha t}, \qquad v_\alpha(\mathbf{r},t) = v_\alpha(\mathbf{r})e^{-i\omega_\alpha t}, \tag{2.24}$$

where the quasiparticle eigenfrequencies ω_α are required to be real valued. Substitution of the trial in Eq. (2.20) into Eq. (2.14), yields the Bogoliubov equations for the elementary excitations

$$\begin{pmatrix} \mathcal{L}(\mathbf{r}) & \mathcal{M}(\mathbf{r}) \\ -\mathcal{M}^*(\mathbf{r}) & -\mathcal{L}^*(\mathbf{r}) \end{pmatrix} \begin{pmatrix} u_\alpha(\mathbf{r}) \\ v_\alpha(\mathbf{r}) \end{pmatrix} = \hbar\omega_\alpha \begin{pmatrix} u_\alpha(\mathbf{r}) \\ v_\alpha(\mathbf{r}) \end{pmatrix}, \tag{2.25}$$

which determine the quasiparticle spectrum and the spatial form of the excitations[3].

[3]The excitations with $\omega_\alpha \neq 0$ should be projected orthogonal to the condensate in the sense that $\int d\mathbf{r}\,[\Psi^*(\mathbf{r})u_\alpha(\mathbf{r}) + \Psi(\mathbf{r})v_\alpha(\mathbf{r})] = 0$ [54].

Properties of the Bogoliubov Equations

In addition to the quasiparticle solutions, it is interesting to study so-called *complex modes* which are solutions to Eq. (2.25) with non-real eigenfrequencies. For an interacting system with $g \neq 0$, the coefficient matrix in Eq. (2.25) is not in general Hermitian, which permits their existence. In this sense, complex modes can be argued as resulting from the nonlinearity of the governing equation of motion, Eq. (2.10). However, for such solutions the condition of Eq. (2.22) has to be relaxed. Stationary states that support modes with non-real eigenfrequencies are called *dynamically unstable*, since the amplitude of a small perturbation related to the excitation of a complex mode evolves initially exponentially in time. If all eigenfrequencies of a stationary state are real, the state is called *dynamically stable.* Dynamical stability of multiquantum vortex states and vortex clusters in different trap geometries is studied in detail in Papers III and IV, respectively. Each solution to Eq. (2.25) satisfies

$$(\omega_\alpha - \omega_\alpha^*) \int d\mathbf{r} \left[|u_\alpha(\mathbf{r})|^2 - |v_\alpha(\mathbf{r})|^2 \right] = 0, \tag{2.26}$$

implying that the norm of solutions corresponding to non-real eigenfrequencies vanishes. For this reason, we normalize the complex modes according to

$$\int d\mathbf{r} \left[|u_\alpha(\mathbf{r})|^2 + |v_\alpha(\mathbf{r})|^2 \right] = 2 \int d\mathbf{r}\, |u_\alpha(\mathbf{r})|^2 = 1. \tag{2.27}$$

By using the Gross-Pitaevskii equation, Eq. (2.11), it is straightforward to verify that $\big(\omega_\alpha; u_\alpha, v_\alpha\big) = \big(0; c\Psi, -c\Psi^*\big)$, for an arbitrary complex number c, satisfies Eq. (2.25). However, this solution merely changes the overall phase of the order parameter $\Psi(\mathbf{r})$, and hence does not correspond to a physical excitation. The coefficient matrix $\mathcal{B}$ of the Bogoliubov equations is related to its Hermitian conjugate by a unitary transformation $\sigma_z \mathcal{B} \sigma_z^{-1} = \mathcal{B}^\dagger$, which implies that if ω_α is an eigenvalue, then also ω_α^* is an eigenvalue. Moreover, the Bogoliubov equations possess the following symmetry: If $\big(\omega_\alpha; u_\alpha, v_\alpha\big)$ is a solution, then $\big(-\omega_\alpha^*; v_\alpha^*, u_\alpha^*\big)$ is also a solution. For modes with real eigenfrequency ω_α, this implies that for every excitation with energy $\hbar\omega_\alpha$ and norm $\int d\mathbf{r} \left[|u_\alpha|^2 - |v_\alpha|^2 \right]$, there exists a solution with energy $-\hbar\omega_\alpha$ and norm $-\int d\mathbf{r} \left[|u_\alpha|^2 - |v_\alpha|^2 \right]$. However, the existence of a solution with a negative norm contradicts the normalization criterion of Eq. (2.22). Furthermore, the excitation spectrum must be bounded from below, and therefore we neglect the solutions with negative norms as unphysical.

Diagonalized Hamiltonian

By inserting the decomposition of Eq. (2.13) into the Hamiltonian, Eq. (2.8), we obtain to second order in the fluctuation $\hat{\phi}(\mathbf{r}, t)$

$$\hat{K} = E(\Psi) + \hat{K}^{(2)}, \tag{2.28}$$

where the zeroth-order term represents the free energy of the stationary state $\Psi(\mathbf{r})$

$$E(\Psi) = \int d\mathbf{r} \left[\Psi^*(\mathbf{r}) \left(\hat{h} - \mu \right) \Psi(\mathbf{r}) + \frac{g}{2} |\Psi(\mathbf{r})|^4 \right], \tag{2.29}$$

the first order term vanishes due to Eq. (2.11), and the second order term is given by

$$\hat{K}^{(2)} = \sum_\alpha \mathrm{Re}(\hbar\omega_\alpha) e^{2\mathrm{Im}(\omega_\alpha)t} \int d\mathbf{r} \left[|u_\alpha(\mathbf{r})|^2 - |v_\alpha(\mathbf{r})|^2 \right] \hat{b}_\alpha^\dagger \hat{b}_\alpha, \tag{2.30}$$

where we have omitted a constant term arising from the commutator of the quasiparticle operators $\hat{b}_\alpha^\dagger$ and $\hat{b}_\alpha$. From this second-order term two profound observations can be made: Firstly, the excitation of a mode α with real eigenfrequency changes the free energy of the state by $\Delta E = \hbar\omega_\alpha$. Hence, the existence of modes with negative eigenfrequencies renders the state *energetically unstable*[4], as the system can lower its free energy by exciting such modes. If all eigenfrequencies of a stationary state are non-negative, the state is called *energetically stable*. Secondly, since the expression $\int d\mathbf{r} \left[|u_\alpha(\mathbf{r})|^2 - |v_\alpha(\mathbf{r})|^2 \right]$ vanishes for complex modes, it costs no energy to excite a mode with a non-real eigenfrequency.

2.5 Finite Temperature Hartree-Fock-Bogoliubov Mean-Field Theory

At finite temperatures, $T \lesssim T_{\mathrm{BEC}}$, the effect of the noncondensate component has to be taken into account in the equation of motion for the condensate wave function.

[4] Energetic stability is also referred to as static stability [55] or local stability [56].

The presence of the thermal cloud affects the stationary states, the elementary excitations, and the dynamics of the system [57, 58]. By taking the expectation value of Eq. (2.9) and using Eq. (2.7), we obtain

$$i\hbar\frac{\partial}{\partial t}\Psi = \left[\hat{h}_\Omega - \mu + g|\Psi|^2\right]\Psi + 2g\Psi\langle\hat{\phi}^\dagger\hat{\phi}\rangle + g\Psi^*\langle\hat{\phi}\hat{\phi}\rangle + g\langle\hat{\phi}^\dagger\hat{\phi}\hat{\phi}\rangle, \tag{2.31}$$

where $\langle\hat{\phi}^\dagger\hat{\phi}\rangle$ is the density of the noncondensate, and $\langle\hat{\phi}\hat{\phi}\rangle$ is the so-called anomalous density which accounts for the effect of the condensate to the collisions among the thermal particles [59]. In the so-called Popov approximation, the anomalous density is neglected [57, 60]. The triple operator product in Eq. (2.31) can be treated in a self-consistent mean-field approximation $\hat{\phi}^\dagger\hat{\phi}\hat{\phi} \simeq 2\hat{\phi}\langle\hat{\phi}^\dagger\hat{\phi}\rangle + \hat{\phi}^\dagger\langle\hat{\phi}\hat{\phi}\rangle$, implying the generalized time-dependent Gross-Pitaevskii equation for the order parameter in the Popov approximation

$$i\hbar\frac{\partial}{\partial t}\Psi = \left[\hat{h}_\Omega - \mu + g\left(|\Psi|^2 + 2\langle\hat{\phi}^\dagger\hat{\phi}\rangle\right)\right]\Psi. \tag{2.32}$$

In a similar manner as in the previous section, we may derive the Bogoliubov equations in the finite temperature scheme, and in the Popov approximation the result is of the same form as in Eq. (2.25) with $\mathcal{L}(\mathbf{r})$ replaced by $\mathcal{L}'(\mathbf{r}) = \mathcal{L}(\mathbf{r}) + 2\langle\hat{\phi}^\dagger\hat{\phi}\rangle\Psi$ [57]. By using the Bogoliubov transformation, Eq. (2.20), it can be shown that the noncondensate density is related to the quasiparticle wave functions and eigenfrequencies through

$$\langle\hat{\phi}^\dagger\hat{\phi}\rangle = \sum_\alpha \left[|u_\alpha|^2 + |v_\alpha|^2\right] f^0(\hbar\omega_\alpha) + |v_\alpha|^2, \tag{2.33}$$

where $f^0(\epsilon_\alpha) = \langle\hat{b}_\alpha^\dagger\hat{b}_\alpha\rangle = 1/(e^{\epsilon_\alpha/kT} - 1)$ is the Bose distribution function. Equations (2.25), with $\mathcal{L} \to \mathcal{L}'$, (2.32), and (2.33) constitute the Hartree-Fock-Bogoliubov-Popov formalism, which was used in Paper II for studying the precession of off-centered vortices at finite temperatures. The equations have to be solved self-consistently by starting, *e.g.*, from the ideal gas case, $g = 0$, and by iterating until self-consistency [57]. Unlike the full HFB formalism, the HFB-Popov theory yields a gapless spectrum and is free of infrared divergencies [54], and hence it is often used in numerical calculations at finite temperatures [27]. The theory is assumed to be accurate for low and intermediate temperatures, $T \lesssim 0.6\ T_{\mathrm{BEC}}$, and for condensate fractions of $0.5 \lesssim N_0/N \lesssim 1$ [61].

3 Vortices in Dilute Scalar Condensates

The fundamental distinction between superfluids and everyday normal fluids is that a superfluid can support dissipationless particle flow analogously to superconductors being able to support dissipationless electric currents. A stable quantized vortex state is an example of such a persistent particle flow, the existence of which has been considered to be a direct manifestation of superfluidity [62]. A quantized vortex line is a one-dimensional singularity in the complex phase of the order parameter. In this chapter, we discuss the structure and stability of quantized vortices in dilute Bose-Einstein condensates in the ultralow temperature limit. For a thorough review of the theory of vortices in trapped dilute Bose-Einstein condensates, see Ref. [63], and of vortices in multicomponent condensates, see Ref. [64].

3.1 Vortex State

For studying the hydrodynamics of a condensate, it is often useful to write the order parameter in the form $\Psi(\mathbf{r}) = f(\mathbf{r})e^{iS(\mathbf{r})}$, where $f(\mathbf{r})$ and $S(\mathbf{r})$ are real-valued functions, and the particle density is related to the amplitude through $n(\mathbf{r}) = f^2(\mathbf{r})$. Analogously to the single-particle case, the particle current density in a state described by a macroscopic wave function is given by

$$\mathbf{j}(\mathbf{r}) = \frac{\hbar}{m}\mathrm{Im}\left[\Psi^*(\mathbf{r})\nabla\Psi(\mathbf{r})\right] = n(\mathbf{r})\frac{\hbar}{m}\nabla S(\mathbf{r}), \tag{3.1}$$

implying that the velocity field $\mathbf{v}(\mathbf{r}) = \mathbf{j}(\mathbf{r})/n(\mathbf{r})$ is proportional to the gradient of the complex phase of the order parameter. Hence, the velocity field in the condensate region must be irrotational, $\nabla \times \mathbf{v}(\mathbf{r}) = 0$, which severely constrains the flow of the condensate. One possible structure that fulfills the requirement of irrotationality is a quantized vortex.

An axisymmetric vortex state is of the form

$$\Psi(\mathbf{r}) = f(r, z)e^{i\kappa\phi}, \tag{3.2}$$

where (r, ϕ, z) are the cylindrical coordinates and $f(r, z)$ is a real-valued function. Because the wave function has to be continuous, it follows that the amplitude of the order parameter has to vanish at the vortex core, $\psi(0,z)=0$, and the parameter κ must be an integer. The parameter κ is called the quantum number, or the winding number, of the vortex: For $|\kappa|=1$, the state in Eq. (3.2) is called a singly quantized vortex state, and for $|\kappa|\geq 2$, a multiply quantized vortex state. Using Eq. (3.1), we find that the velocity field associated with axisymmetric vortex states is of the form

$$\mathbf{v}(\mathbf{r})=\frac{\hbar}{m}\frac{\kappa}{r}\mathbf{e}_\phi, \tag{3.3}$$

with the unit vector $\mathbf{e}_\phi=\partial_\phi\mathbf{r}/||\partial_\phi\mathbf{r}||$. Thus, the particles are rotating about the vortex core where the particle density vanishes, and the circulation, defined by the line integral of the velocity field about the core, is quantized in units of h/m, in which h is Planck's constant. A typical length scale of the vortex core region is given by the healing length $\xi=1/\sqrt{8\pi na}$ which essentially describes the distance over which the order parameter regains its bulk value when perturbed locally.

The axisymmetric vortex state yields a simple picture of the most important aspects of the structure of a vortex line. However, it has been shown that for fast enough rotation even in a completely axisymmetric trap geometry, the ground state of the system hosts a bent vortex line for an elongated condensate [65,66]. Another important example of a curved vortex is the vortex ring which can be viewed as a vortex line closed upon itself.

The Gross-Pitaevskii and Bogoliubov Equations for Axisymmetric Vortex States

In a cylindrically symmetric configuration, the Gross-Pitaevskii and Bogoliubov equations, Eqs. (2.11) and (2.25), may be cast in a simpler form. For a stationary state of the form presented in Eq. (3.2), the Gross-Pitaevskii equation reduces to $\mathcal{L}'_\kappa(r,z)f(r,z)=0$, in which

$$\mathcal{L}'_\kappa(r,z)=-\frac{\hbar^2}{2m}\left[\frac{1}{r}\frac{\partial}{\partial r}+\frac{\partial^2}{\partial r^2}-\frac{\kappa^2}{r^2}+\frac{\partial^2}{\partial z^2}\right]+V_{\mathrm{ext}}(r,z)-\mu+gf^2(r,z), \tag{3.4}$$

in the non-rotating frame of reference. It is convenient to write the quasiparticle wave functions in the form $u_q(\mathbf{r})=u_q(r,z)e^{i(\kappa_q+\kappa)\phi}$ and $v_q(\mathbf{r})=v_q(r,z)e^{i(\kappa_q-\kappa)\phi}$, where κ_q is an integer that specifies the angular momentum of the quasiparticle excitation with respect to the condensate. By substituting these forms into the

Bogoliubov equations, we obtain

$$\begin{pmatrix} \mathcal{L}_{\kappa_q+\kappa}(r,z) & M(r,z) \\ -M(r,z) & -\mathcal{L}_{\kappa_q-\kappa}(r,z) \end{pmatrix} \begin{pmatrix} u_q(r,z) \\ v_q(r,z) \end{pmatrix} = \hbar\omega_q \begin{pmatrix} u_q(r,z) \\ v_q(r,z) \end{pmatrix}, \tag{3.5}$$

where $\mathcal{L}_\kappa(r,z) = \mathcal{L}'_\kappa(r,z) + gf^2(r,z)$, and $M(r,z) = gf^2(r,z)$. It is worthwhile to notice that the coefficient matrix in Eq. (3.5) is real. Hence, if $(\omega_q; u_q, v_q)$ is a solution, then $(\omega_q^*; u_q^*, v_q^*)$ is also a solution.

3.2 Energetic Stability of Stationary Vortex States

Multiply quantized vortex states are in general energetically unstable[5]. Let us consider, for example, two vortex lines with quantum numbers κ_1 and κ_2 in a condensate confined in a cylindrical vessel of radius R. The energy per unit length associated with the vortices located close to the center of the cylinder is given, within logarithmic accuracy, by

$$E_{\kappa_1,\kappa_2} = \frac{\pi n\hbar^2}{m}\left[(\kappa_1^2+\kappa_2^2)\log\frac{R}{\xi} + 2\kappa_1\kappa_2\log\frac{R}{d}\right], \tag{3.6}$$

for $\xi \ll d \ll R$, in which d is the separation of the vortex lines [62]. The first term in the brackets is the kinetic energy of the azimuthal flow, and the second term is the interaction energy of the vortex lines. Because $E_{\kappa,0} > E_{\kappa-1,1}$, for a given total circulation of $\kappa h/m$, it is energetically favorable to have a collection of κ singly quantized vortices compared to one κ-quantized vortex.

In non-rotating harmonic traps, the quasiparticle energy spectra of stationary axisymmetric single quantum vortex states contain at least one negative excitation energy in the zero-temperature limit [28, 68, 69], and therefore these states are energetically unstable. This so-called *anomalous mode* corresponds to transversal displacement of the vortex which eventually spirals out of the condensate if dissipation is present in the system [56]. However, the state can be stabilized by rotation of the external potential: In the rotating frame the free energy per particle in the singly quantized vortex state is of the form $E_\Omega = E_0 - \Omega L_z = E_0 - \hbar\Omega$, where we

[5] Multiply quantized vortices may, in some cases, be energetically favorable. For example, the doubly quantized vortex in a rapidly rotating quartic potential can be made energetically stable [67].

have assumed that the vortex line coincides with the rotation axis, and denoted the free energy per particle in the non-rotating frame by E_0 and the angular momentum per particle along the rotation axis by L_z. Figure 3.1 illustrates the stabilization of the singly quantized vortex in a rotating potential. The curves in the figure represent qualitatively the free energy of the state with respect to the displacement of the vortex from the center of the trap [69, 70]. Above the critical rotation frequency Ω_m, the axisymmetric vortex state becomes a local minimum of the free energy, rendering the state robust against small displacements of the vortex from the center. However, the free energy of the nonvortex state is still the global minimum of the free energy below the critical angular velocity Ω_{c1}, and thus for rotation frequencies $\Omega_m < \Omega < \Omega_{c1}$ the vortex state is *metastable*. The energy barrier, denoted by ΔE_Ω in Fig. 3.1, prevents the vortex from moving out of the condensate. For $\Omega > \Omega_{c1}$, the vortex state becomes *thermodynamically stable* as the global minimum of the free energy [71], and in this case the energy barrier ΔE_Ω prevents a vortex from entering the system. For a higher rotation frequency Ω_{c2}[6], the barrier vanishes or becomes negligible compared to other energy scales in the system [73]. Hence, a vortex can be spontaneously nucleated by rotating the external potential with a frequency $\Omega > \Omega_{c2}$. When the rotation frequency is increased further, the single quantum vortex state becomes energetically unfavorable against states with two or more vortices, which is discussed in Sec. 4.2.

3.3 Off-Centered Vortices

Understanding the behavior of off-centered vortices in harmonically trapped Bose-Einstein condensates is important, because an energetically unstable axisymmetric vortex tends to become off-centered in the presence of dissipation. Moreover, under sufficient external rotation, vortices emerge from the periphery of the cloud. It has been shown theoretically that for small displacements of the vortex from the center of the trap, the vortex moves perpendicular to the local gradient of the potential [69]. In a cylindrically symmetric potential, a vortex precesses along a circular constant-

[6] The critical frequency Ω_{c2} is given by the Landau criterion for formation of surface excitations [72].

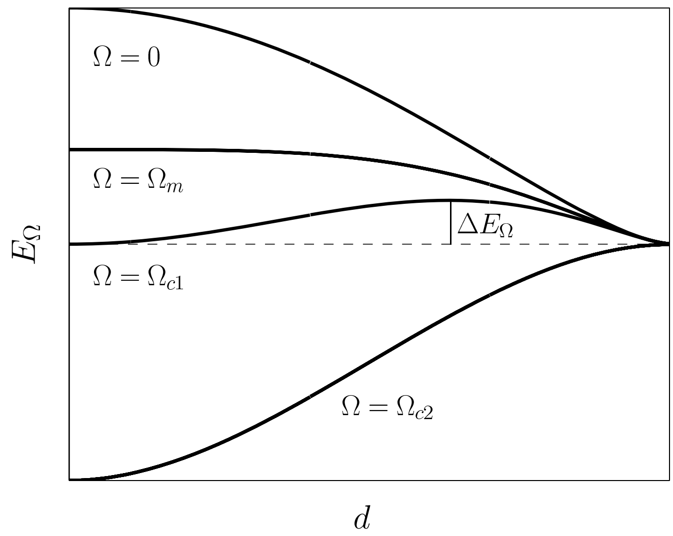

Figure 3.1: Qualitative dependence of the free energy E_Ω on the displacement d of the vortex from the center. The free energy barrier ΔE_Ω depends on the rotation frequency of the trapping potential Ω, and becomes negligible at the critical velocity Ω_{c2}.

energy path. This can be viewed as resulting from the Magnus effect: A singly quantized vortex line moving with velocity v experiences an effective force per unit length, $F = nhv$, directed towards the center of the trap. Precession of off-centered vortices has been observed experimentally, and their precession frequencies have been measured [74].

In Papers I and II, we have studied the excitations of off-centered vortex states in harmonic traps at zero and finite temperatures, respectively. When the external potential is rotated with an angular velocity satisfying $\Omega_m < \Omega < \Omega_{c2}$, in addition to the axisymmetric vortex state, there exist off-centered vortex states with a very weak time-dependence in the rotating frame of reference in which the external potential is stationary. In these states the vortex is displaced from the center of the trap such that it is located on top of the free energy barrier, denoted by ΔE_Ω in Fig. 3.1. In the laboratory frame, the vortex precesses around the center of the condensate with a frequency that coincides with the angular velocity of the trap. In these papers, we study an effectively two-dimensional condensate and look for solutions to the time-dependent Gross-Pitaevskii equation, Eq. (2.10), which satisfy[7]

$$\max_{x,y}|\partial_t\psi(x,y,t)|/\max_{x,y}|\psi(x,y,t)| < 0.0005\ \omega_{\rm trap}, \tag{3.7}$$

where x and y are the cartesian coordinates, and $\omega_{\rm trap}$ is the trapping frequency. The dimensionless angular momentum per particle $L = \langle\hat{L}\rangle/(N\hbar)$ of the off-centered vortex state varies smoothly as a function of the vortex displacement d. This follows closely the analytical result based on the Thomas-Fermi approximation[8], $L_{\rm TF} = [1-(d/R_{\rm TF})^2]^2$ [75], where $R_{\rm TF}$ is the Thomas-Fermi radius of the condensate, see Fig. 1 (b) in Paper I. Also, the normalized energy $\Delta E' = (E-E_0)/(E_1-E_0)$, is given quite accurately by the Thomas-Fermi result, $\Delta E'_{\rm TF} = [1-(d/R_{\rm TF})^2]^{3/2}$ [63], as shown in Fig. 1 (c) in Paper I. Here E, E_1, and E_0 are the energies of the off-centered vortex, centered vortex, and vortexfree states, respectively.

For the weakly time-dependent states, we solve the Bogoliubov equations, as if they were stationary states. For all trap rotation frequencies considered, the excitation spectrum contains a mode with a negative excitation energy in the rotating frame of reference, and therefore the off-centered vortex states are energetically unstable. In the limit of small displacements, however, the excitation energy approaches zero. In the finite temperature calculations, the Bogoliubov equations are solved using the self-consistent Hartree-Fock-Bogoliubov-Popov scheme, *c.f.* Sec. 2.5. Above a chosen energy cutoff, the excitations are taken into account within a semiclassical approximation [72, 76, 77]. It has been shown that within the Popov approximation, the noncondensate stabilizes a centered vortex at finite temperatures [78] and even in the ultralow temperature limit [79], which is in agreement with the results obtained in Paper II. In the zero temperature limit, it can be shown that for small displacements the direction of precession of an off-centered vortex in a frame rotating with the trap is related to the sign of the lowest excitation energy [80]: For $\Omega < \Omega_m$, the excitation energy is negative and the vortex precesses in the counterclockwise direction, and vice versa for $\Omega > \Omega_m$. However, the results of Paper II show that this relationship is not valid at finite temperatures within the Popov approximation.

[7]For vortices very close to the surface of the condensate, the right-hand side of this condition is relaxed to 0.03 $\omega_{\rm trap}$.

[8]In these calculations the Thomas-Fermi approximation is well satisfied.

3.4 Dynamical Stability of Multiply Quantized Vortex States

Energetic stability always implies dynamical stability, but not necessarily vice versa. Even though multiply quantized vortices in harmonic traps are energetically unfavorable, such states might still be robust against small perturbations. In Paper III, we have studied the dynamical stability of multiply quantized vortex states[9], Eq. (3.2), with $2 \leq \kappa \leq 4$. The external cylindrically symmetric potential employed in the work was of the form

$$V_{\mathrm{ext}}(r, z) = \frac{1}{2} m\omega_r^2 \left(r^2 + \lambda^2 z^2\right), \tag{3.8}$$

in the cylindrical coordinates (r, φ, z). The parameter $\lambda = \omega_z/\omega_r$ determines the geometry of the trap, where ω_r and ω_z measure the strengths of the radial and axial confinements, respectively. If $\lambda \ll 1$, the radial confinement is much stronger than the axial, and in such a configuration the BEC in its ground state is called cigar-shaped. On the other hand, in a configuration where $\lambda \gg 1$, the BEC is called pancake-shaped. From previous theoretical studies it is known that, for example, the doubly quantized vortex is dynamically unstable in the cigar-shaped limit [82], see also Sec. 4.3 and Paper V. Moreover, in pancake-shaped condensates the multiquantum vortex state can be dynamically stable or unstable depending on the interaction strength g [83, 84]. In this work, we investigated the dynamical stability of multiquantum vortex states in various trap geometries, $0 < 1/\lambda \leq 2$, and for various effective interaction strengths[10], $0 \leq \tilde{g} \leq 1000$, by solving the Bogoliubov equations for axisymmetric vortex states, Eq. (3.5). Figure 3.2 displays, for the doubly quantized vortex state, the absolute value of the imaginary part of the dominating instability eigenfrequency, $\max_q |\mathrm{Im}(\omega_q)|$, with respect to the aspect ratio λ and the effective interaction strength $\tilde{g}$. In the white regions all the eigenfrequencies are real, and hence in these regions the system is dynamically stable. In the pancake-shaped limit, the quasiperiodic structure of the instability as a function of the interaction strength $\tilde{g}$ is restored, *c.f.* Refs. [83, 84]. Towards the cigar-shaped limit, the instability regions start to overlap, and eventually the system becomes

[9] See also Ref. [81].

[10] In this case, the effective interaction strength $\tilde{g}$ is related to the s-wave scattering length a by $\tilde{g} = 4\pi a N/a_r$, where $a_r = \sqrt{\hbar/(m\omega_r)}$ is the harmonic oscillator length.

dynamically unstable for all interaction strengths. However, in the intermediate regions, *e.g.*, for spherically symmetric configurations, there exist wide regions of dynamical stability in which the lifetime of the multiquantum vortex state should be significantly longer.

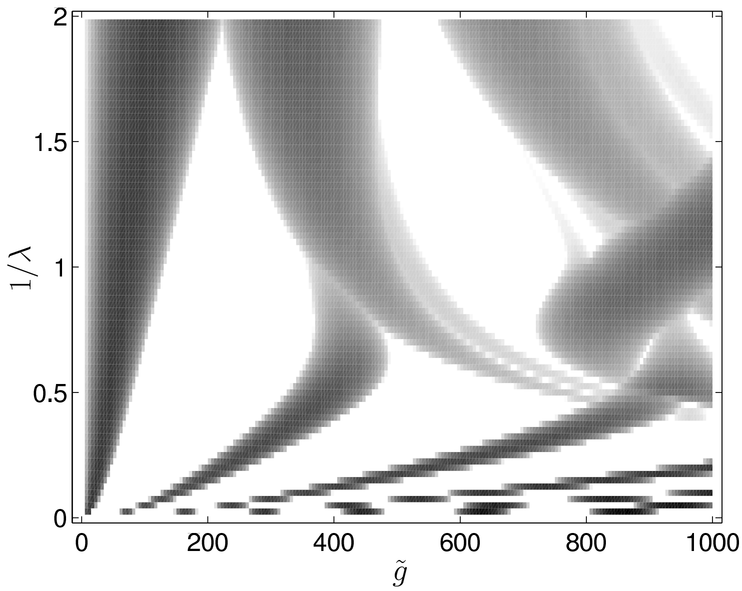

Figure 3.2: Regions of dynamical stability (white) for the stationary doubly quantized vortex state in the aspect ratio – interaction strength -parameter plane.

3.5 Stationary Vortex Clusters

In Paper IV, we have studied the dynamical stability of stationary vortex cluster states in dilute pancake-shaped BECs in non-rotating harmonic traps[11]. The clusters consist of vortices and anti-vortices in specific configurations such that the forces on the vortices and anti-vortices balance exactly and the state is stationary. For vortices the winding number κ is positive and for anti-vortices negative. Two vortices with winding numbers of the same sign repel each other and vortices with winding numbers of the opposite sign feel an attractive force, see Eq. (3.6). Figure 3.3

[11]Note that the symbols κ_q and λ are used in different contexts in Papers III and IV.

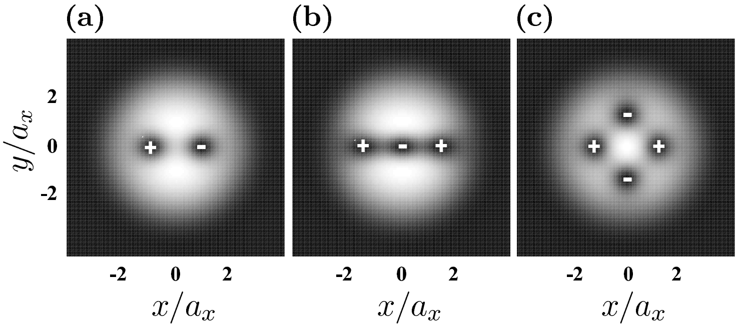

Figure 3.3: Density profiles of three stationary vortex clusters in a cylindrically symmetric harmonic trap: (a) the vortex dipole, (b) the vortex tripole, and (c) the vortex quadrupole. The core of a vortex is marked by '+' and an anti-vortex by '–'. Length is measured in units of the harmonic oscillator length $a_x = \sqrt{\hbar/(m\omega_x)}$. The vortex dipole and quadrupole were originally discovered by Crasovan *et al.* [85, 86], and the vortex tripole by Möttönen *et al.* [87].

shows the density profiles of the three vortex clusters whose energetic and dynamical stability was studied. The stationary states were solved using the Gross-Pitaevskii equation, Eq. (2.11), with an external potential of the form

$$V_{\text{ext}} = \frac{1}{2}m\left(\omega_x^2 x^2 + \omega_y^2 y^2 + \omega_z^2 z^2\right), \tag{3.9}$$

where $\omega_x, \omega_y \ll \omega_z$, for different anisotropy parameters $\lambda = \omega_x/\omega_y$ and effective interaction strengths $\tilde{g}$. For $\lambda = 1$, the stationary vortex quadrupole was found to exist for all positive interaction strengths, whereas the dipole and tripole were found to exist only when $\tilde{g} \gtrsim 42$ and $\tilde{g} \gtrsim 108$, respectively. In order to determine the stability of each stationary state, we solved the Bogoliubov equations, Eq. (2.25). Negative energy excitations exist for each of the clusters, implying energetic instability. In rotationally symmetric traps, all of the three clusters have at least the dynamical instability mode corresponding to rigid rotation of the configuration. Moreover, the dipole mode has another instability mode, corresponding to annihilation of the cluster, for $50 \lesssim \tilde{g} \lesssim 80$, the quadrupole for $50 \lesssim \tilde{g} \lesssim 280$, and the tripole for all values of $\tilde{g}$. Temporal evolution of the dipole and quadrupole states shows revival of the collapsed configuration close to the initial state.

4 Experiments with Vortices in Dilute Bose-Einstein Condensates

After the realization of a nearly ideal Bose-Einstein condensate, one of the big challenges was to observe quantized vortices in the system. A successful experiment would yield unambiguous evidence of Bose-Einstein condensation and the existence of a macroscopic wave function. Measurements concerning the vortex structure, stability, and dynamics would provide stringent tests to the underlying many-body quantum field theory. In superfluid helium, the quantization of circulation was observed in 1958 by V. F. Vinen [88, 89], and vortices were observed in 1979 by E. J. Yarmchuk *et al.* [42].

4.1 Trapping of Alkali Atoms With Magnetic Fields

In a typical experiment a beam of atoms is directed into a so-called Zeeman slower, in which the velocity of the atoms is reduced enough to be captured in a magneto-optical trap (MOT). The atom vapour is laser cooled down to sub mK temperature, cold enough to be captured purely magnetically. Condensation is finally achieved by cooling the vapour below the transition temperature T_{BEC} by forced evaporative cooling, in which the most energetic atoms are removed from the trap with radio-frequency transitions.

Trapping of neutral atoms with a magnetic field is possible because of the Zeeman effect: The energy of an atom in a given state in a weak magnetic field is of the form

$$E = E_0 - \mu B, \tag{4.1}$$

where E_0 is the energy in the absence of the magnetic field B, and μ is the magnetic moment of the atom along the magnetic field in the particular state. Hence, in an inhomogeneous field, the atom feels a spatially varying potential. Generally, it is not possible for the strength of a static magnetic field to have local maxima, but it can contain a local minimum. Therefore, in order to trap atoms, they have to be in a weak-field seeking state, *i.e.*, their magnetic moment must be oriented opposite to the direction of the magnetic field.

The first condensate was achieved in a time-averaged orbiting potential (TOP) trap, which consists of a quadrupole field and a uniform field rotating at a constant angular frequency [90], resulting in a harmonic time-averaged potential. Another commonly used configuration which provides the atoms a harmonic confinement is the Ioffe-Pritchard trap. One design of the latter consists of two Helmholtz coils with currents flowing in the same direction and four leads, known as the Ioffe bars. Let us fix the coordinate axes such that the coils lie parallel to the x-y plane, separated by some distance, and the z-axis coincides with the centers of the coils. The Ioffe bars lie parallel to the z-axis, symmetrically in each quadrant of the x-y plane, with currents flowing in the opposite directions in neighboring wires. Close to the origin, the magnetic fields generated by the coils and the wires are given by [53]

$$\mathbf{B}_{\text{coils}} = \left[-B_z - 3C_1\left(z^2 - \frac{1}{2}r^2\right)\right]\mathbf{e}_z + 3C_1 zr\mathbf{e}_r, \tag{4.2}$$

$$\mathbf{B}_{\text{bars}} = C_2 x\mathbf{e}_x - C_2 y\mathbf{e}_y, \tag{4.3}$$

where B_z, C_1, and C_2 are constant depending on the geometry and the currents: B_z is the strength of the axial bias field, C_1 determines the curvature of the axial field, and C_2 characterizes the strength of the field generated by the Ioffe bars. Assuming that $B_z, C_1 > 0$, the total magnetic field strength is of the harmonic form

$$B = B_z + 3C_1\left(z^2 - \frac{1}{2}r^2\right) + \frac{C_2^2}{2B_z}r^2, \tag{4.4}$$

to second order in the coordinates. The field has a local minimum at the origin provided that $C_2^2 > 3B_zC_1$.

4.2 Methods to Create Vortices

In this section, we will briefly sketch methods to create singly quantized vortices, vortex lattices, and multiquantum vortices in dilute Bose-Einstein condensates. In addition to the methods described below, vortices have been created by moving laser beams [91, 92], and by transferring orbital angular momentum into a condensate from a Laguerre-Gaussian laser beam [93]. Vortices and vortex rings have also been observed as a result of decay of solitons [94, 95]. Moreover, M. Möttönen *et al.* have recently suggested a method for creating a vortex with an arbitrarily large winding number by pumping vorticity adiabatically into a condensate with external magnetic fields [96].

Vortex in a Two-Component Condensate

The first quantized vortices in dilute atomic Bose-Einstein condensates were created by Matthews *et al.* in 1999 [40], using a method proposed by Williams *et al.*, based on transferring matter between two hyperfine states of the atoms [97]. The method relies on mechanical rotation of the system and coupling of two hyperfine states with an electric field: The two components of the condensate are confined in harmonic potentials with a common trapping frequency. The centers of the harmonic potentials are spatially shifted by adding a linear potential yielding an energy shift to the components equal in magnitude but of the opposite sign. The two harmonic potentials are rotated about their symmetry axis at a frequency $\omega_{\rm rot}$ by rotating the linear potential. The population transfer between the states is driven with an off-set laser beam, detuned by a frequency δ from resonant coupling. In the frame of reference in which the potentials are static, the single-particle Hamiltonians of the two components are of the form $H_0 - \omega_{\rm rot}\hat{L}_z^{(i)}$, where $\hat{L}_z^{(i)}$ is the angular momentum per particle of the ith component along the rotation axis. Hence, the population transfer between a nonvortex state with $\langle \hat{L}_z \rangle = 0$ in one component and a vortex state with $\langle \hat{L}_z \rangle = \hbar$ in the other becomes resonant if the detuning is canceled by the energy difference of the states, $\delta \approx \omega_{\rm rot}$[12]. The direction of the particle flow in the vortex state is not directly associated with the rotational motion of the potentials: a vortex with the same quantum number is obtained by reversing the direction of the mechanical rotation and the sign of the detuning δ.

In the experimental realization of this method, the two components consist of the hyperfine states $|F=1, m_F=-1\rangle$ and $|F=2, m_F=1\rangle$ of ^{87}Rb. The condensate is confined in a time-averaged orbiting potential magnetic trap yielding identical harmonic potentials for the two states. The mechanical rotation is attained with a detuned focused laser beam rotating around the condensate, providing a time-

[12]In fact, the relatively small difference in the chemical potentials of the vortex and the nonvortex state should also be included.

dependent ac Stark shift. The population transfer between the internal states is induced by a pulsed two-photon microwave field. Singly quantized vortex states were created in both of the components in the experiment, and differences in their dynamics and stability resulting from the different scattering lengths of the atoms in the components were observed. The vortex cores were clearly distinguishable and their precessional motion was detected. The phase difference between the vortex and the nonvortex states was imaged using a nondestructive state-selective phase contrast imaging [45], suggesting that the vortex state possesses angular momentum.

Generation of Vortex Lattices

At the early stages of vortex experiments, it was not clear whether one could create vortices using an analogy to the rotating bucket experiment with superfluid helium. Coupling of the condensate to the rotating environment was not well understood, and therefore the time scale for creating vortices could well have been longer than the lifetime of the condensate itself [40]. However, soon after the first successful vortex experiment, Madison *et al.* managed to create a condensate containing up to four vortices by stirring it with a focused laser beam [98], see also Refs. [99, 100]. In the experiment, a cigar-shaped condensate of ^{87}Rb is prepared in the $|F = 2, m_F = 2\rangle$ state and confined in a Ioffe-Pritchard trap [11]. The stirring beam creates effectively an anisotropic harmonic potential, which is rotated at a fixed angular frequency Ω about the long axis of the condensate during the evaporative cooling stage. After the vortex creation stage, the stirring beam and the magnetic trap are switched off, allowing the cloud to expand during free fall. After the expansion, the condensate is illuminated with a resonant laser beam and the shadow of the cloud in the beam is imaged onto a CCD camera. Depending on the angular frequency Ω of the stirring beam, up to four vortices were observed in a symmetric arrangement, supporting the predicted signatures of rotating Bose-Einstein condensates [101]. The rotation frequency Ω needed for the formation of one vortex was precisely measured yielding a value much higher than the theoretically predicted value Ω_{c1} for the vortex state to become energetically favorable compared to the nonvortex state [71, 102]. This suggested the existence of the energy barrier ΔE_Ω, see Fig. 3.1. Later on, giant arrays containing over a hundred vortices uniformly distributed in an Abrikosov lattice have been observed [103]. Also, giant vortices containing up to 60 phase singularities have been created in rapidly rotating condensates by suppressing the density at the center of the cloud with a tightly focused resonant laser beam [104].

Creation of Multiply Quantized Vortices

The first multiply quantized vortices were created by using the topological phase imprinting technique [105], originally proposed by Nakahara *et al.* [106], see also Refs. [107–109]. In this method, the phase of the order parameter corresponding to a vortex state is obtained by rotating the spins of the condensed atoms through an angle π about an axis that depends on the location of a particular atom. The atoms are supposed to be confined in a weak-field seeking state $|F, m_F\rangle$ in a Ioffe-Pritchard trap, $\vec{\mathbf{B}}(\mathbf{r}) = x\mathbf{e}_x - y\mathbf{e}_y + B_z\mathbf{e}_z$, in which the curvature of the axial field is neglected, *c.f.* Eqs. (4.2) and (4.3). Initially, the axial field B_z is assumed to be strong compared to the quadrupole field in the condensate region, and hence all the spins lie parallel to the z-axis. The axial field is inverted adiabatically, $B_z \to -B_z$, such that the individual spins follow the local magnetic field[13]. The spin rotation can be described with a unitary transformation of the form [110], $\mathbf{R}_{\hat{n}(\phi)}(\pi) = e^{-i(\hat{F}/\hbar)\cdot\hat{n}(\phi)\pi}$, acting on the components of the order parameter, where $\hat{n}(\phi) = \sin(\phi)\mathbf{e}_x + \cos(\phi)\mathbf{e}_y$ denotes the local direction of rotation. The rotation matrix can be decomposed according to $\mathbf{R}_{\hat{n}(\phi)}(\pi) = e^{i(\hat{F}_z/\hbar)\phi}e^{-i(\hat{F}_y/\hbar)\pi}e^{-i(\hat{F}_z/\hbar)\phi}$. By applying the rotation, one obtains in the laboratory frame [111]

$$\mathbf{R}_{\hat{n}(\phi)}(\pi)|F, m_F\rangle = (-1)^{(F-m_F)}e^{-i2m_F\phi}|F, -m_F\rangle, \tag{4.5}$$

which describes a vortex state with phase winding $\kappa = -2m_F$.

In the experiments, condensates consisting of ^{23}Na were prepared in the hyperfine state $|F = 1, m_F = -1\rangle$ or $|F = 2, m_F = +2\rangle$. The vortices were created by reversing an external axial bias field linearly in time, and the vortices could be removed by reversing the bias field back to its original direction. The density profiles

[13] Some of the atoms are lost due to Majorana spin flips at the center of the trap when the axial field vanishes.

of the vortices were measured using the absorption imaging technique. The angular momentum per particle was measured using surface wave spectroscopy [46, 47, 112]. The results corresponded very accurately to $\langle \hat{L}_z \rangle = 2\hbar$ for the $m_F = -1$ state and $\langle \hat{L}_z \rangle = -4\hbar$ for the $m_F = 2$ state.

4.3 Splitting of Doubly Quantized Vortices

In the experiments of Leanhardt *et al.* [105], no detectable splitting of the multiply quantized vortices was observed, contradicting with theoretical predictions of their instability against decay into singly quantized vortices [62]. In reversing the axial bias field, the local minimum of the magnetic field strength at the center of the condensate transforms into a saddle point, resulting in axial antitrapping of the weak-field seeking state. This limited the lifetime of the system to $\lesssim 50$ ms. The axial absorption images of the vortices were taken $\lesssim 30$ ms after the inversion of the axial field, which is too soon to observe the splitting of the vortices in a condensate with a relative large number of particles. Moreover, the absorption images were taken along the whole length of the condensate, which might lead to blurring of the cores due to bending and intertwining of the vortex lines near the ends of the cloud [65, 66, 82, 113].

The splitting times of doubly quantized vortices in a condensate of ^{23}Na in the $|F = 1, m_F = -1\rangle$ state were measured in a similar setup by Y. Shin *et al.* [114]. The problem with the axial antitrapping of the condensate was overcome by changing the sign of the axial field curvature as B_z passed zero during the creation of the doubly quantized vortex. Also, possible blurring effects resulting from bending and intertwining of the vortex lines near the ends of the cloud were reduced by taking the axial absorption images only from a 30 μm thick slice at the center of the condensate. The splitting times of the doubly quantized vortices were measured for various values of the parameter an_z, where a is the s-wave scattering length and $n_z = \int |\psi(x, y, 0)|^2 dxdy$ is the averaged axial density of atoms at the center of the condensate. The density was controlled by removing a variable number of atoms by radio-frequency evaporation before creating the vortex. After the creation of the vortex, the condensate was held in the trap for a certain time before releasing and

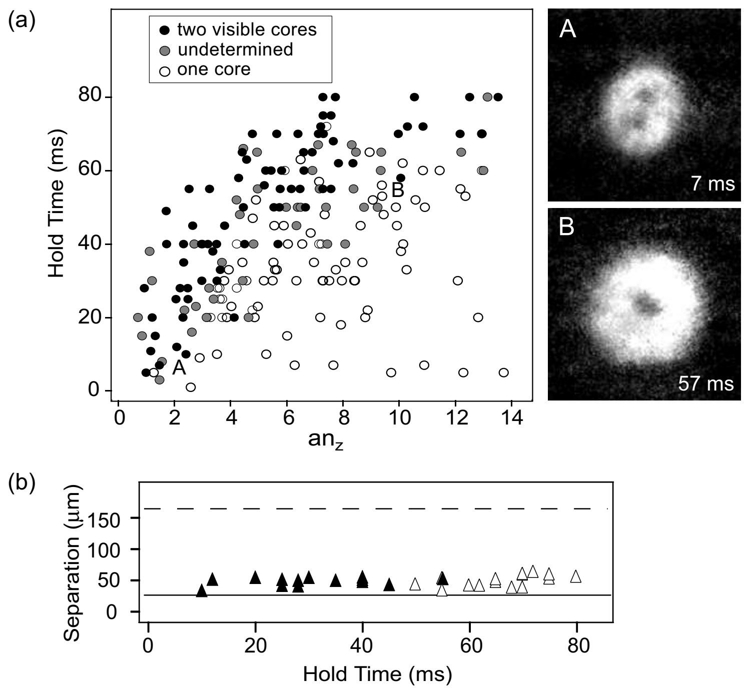

Figure 4.1: (a) Splitting times of doubly quantized vortices with respect to the parameter an_z. The measured density profiles are classified to consist of one minimum (open circle) as in B or two minima (black dot) as in A, corresponding to a doubly quantized vortex or two singly quantized vortices. The cases where the core was elliptical, but the two cores were not clearly resolved are denoted by gray circles. (b) Separation of the single quantum vortex cores as a function of the hold time (Y. Shin *et al.*, 2004).

letting the cloud to expand for 15 ms in order to take the absorption image. Figure 4.1(a) illustrates the measured splitting times of doubly quantized vortices. The splitting time increases with increasing density and seems to saturate for densities higher than $an_z \gtrsim 10$. Figure 4.1(b) shows the separation of the observed single quantum vortex cores as a function of holding time. The distance of the cores is roughly constant, implying that most likely the splitting process is mainly driven by a dynamical instability instead of dissipation: The latter would lead to gradual increase in the separation of the cores.

In order to elucidate the role of the dynamical instability in the splitting of the doubly quantized vortices, in Paper V we performed numerical simulations in the

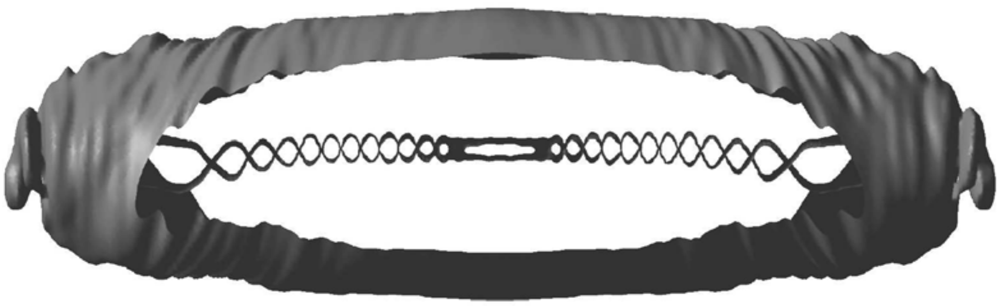

Figure 4.2: Density isosurface of a cigar-shaped Bose-Einstein condensate with a doubly quantized vortex splitting into two singly quantized vortices. The vortex lines intertwine strongly as they split and surface modes are excited during the splitting process.

zero-temperature limit closely mimicking the experimental setup, see also Refs. [82, 115, 116]. The origin of the perturbation which initiates the splitting process lies in the gravitational sag: Initially, when the bias field is strong such that B_z is the dominating term in Eq. (4.4), the gravitational force, directed perpendicular to the axial direction, merely shifts the location of the minimum of the potential. The doubly quantized vortex is created by reversing the axial magnetic field linearly in time, $B_z \rightarrow -B_z$, *c.f.* Sec. 4.2. When the axial field vanishes, the potential becomes linear instead of harmonic in the radial direction, and thus, at this time the gravitational sag vanishes. This vertical kick breaks the rotational symmetry of the system: Due to inertia, the center of mass of the condensate does not follow the minimum of the potential exactly, yielding a sufficient perturbation to initiate the splitting process.

Starting from the axisymmetric doubly quantized vortex state, we solved the time evolution of the condensate, see Fig. 4.2, using the time-dependent Gross-Pitaevskii equation with various values of the parameter an_z, and calculated the axially integrated density profiles as functions of time. From the density profiles, we determined the splitting time T of the doubly quantized vortex, as shown in Fig. 4.3. The splitting times obtained from the simulation agree well with the experimental results, demonstrating the importance of the dynamical instability of the system

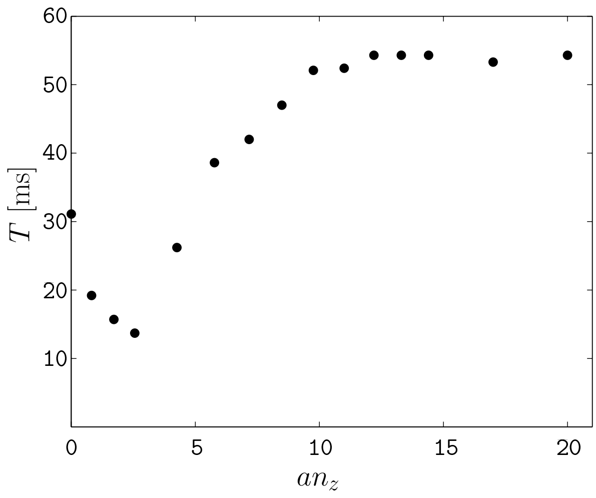

Figure 4.3: Splitting time T of a doubly quantized vortex as a function of the parameter an_z.

in the splitting process. In Ref. [115], the same experiment was analyzed from a different point of view: It was claimed that the splitting process was mainly driven by thermal fluctuations. A fraction of 10–15 % of thermal atoms yielded a time scale comparable to that in the experiment. However, the splitting times obtained from the zero-temperature simulations performed in Paper V are somewhat shorter than the experimental results, verifying that the effect of dissipation does not have to be taken into account in their interpretation.

4.4 Splitting of Quadruply Quantized Vortices

It is known from numerical simulations that, in a harmonic trap, the doubly quantized vortex state with $\kappa = 2$ can have a dynamical instability mode only for $\kappa_q = 2$ in Eq. (3.5). A vortex with a higher quantum number, such as the quadruply quantized vortex with $\kappa = 4$, can have several dynamical instability modes, *e.g.*, for $\kappa_q = 2$, 3, 4, 5, and 6, each mode corresponding to a κ_q-fold symmetric splitting pattern [84]. The imaginary parts for modes with $\kappa_q > \kappa$ are greatly suppressed compared to the modes with $\kappa_q \leq \kappa$. For example, the 5-fold symmetric splitting pattern of an axisymmetric quadruply quantized vortex corresponds to splitting into five singly quantized vortices and a singly quantized anti-vortex.

In Paper VI, we studied the splitting of a quadruply quantized vortex into four singly quantized vortices both experimentally and theoretically. In the series of experiments, a cigar-shaped BEC consisting of ^{87}Rb atoms was prepared in the $|F = 2, m_F = 2\rangle$ state in a Ioffe-Pritchard trap [117]. The quadruply quantized vortex was created by reversing the axial magnetic field, as described in Sec. 4.2. A blue-detuned laser beam was applied below the condensate in order to remove the gravitational sag and consequently to stabilize the formation of the vortex. Time evolution of the vortex was determined by taking a tomographic image of the central region of the condensate after ballistic expansion. The off-centered minimum in the density profile, corresponding to the vortex core area, was observed to precess around the center of the condensate in the counterclockwise direction. Also, the core area was found to deform into a linear shape, rotating around its center.

By slicing the cigar-shaped condensate along the axial direction, it can be roughly viewed as a collection of pancake-shaped clouds. Their central densities are determined by their positions along the axis. In order to explain the deformation of the core into the linear shape, the Bogoliubov spectrum of the pancake-shaped condensate profiles was solved for the averaged axial density an_z relevant in the experiment. Indeed, the $\kappa_q = 2$ mode was found to be the dominating instability mode along the whole length of the cigar-shaped condensate, explaining the two-fold symmetric splitting pattern. Moreover, the time evolution of the condensate was solved using the time-dependent Gross-Pitaevskii equation, for an initial state for which the quadruply quantized vortex was off-centered. This provided further evidence that the linear deformation of the core was due to splitting of the quadruply quantized vortex into four singly quantized vortices which were aligned in a linear configuration.

The precessional motion of the vortex cluster around the center of the condensate is analogous to the precession of a singly quantized vortex, *c.f.* Sec. 3.3. On the other hand, the rotational motion of the linearly shaped defect around its center can be understood by considering the velocity fields of the individual vortices separated by an equal distance: The velocity field at the location of an individual vortex is given by the sum of the fields generated by the other vortices. Hence, a vortex at the end of the chain feels effectively a velocity field built constructively from the fields of the rest of the vortices. At the location of a vortex close to the center of the chain, the velocity fields generated by the neighboring vortices cancel, resulting in a smaller velocity field. This simplified model yields a velocity field which depends roughly linearly on the distance from the center of the chain. The precessional and rotational frequencies observed in the experiment matched reasonably well with the frequencies obtained from the simulation.

5 Tunneling of Bose-Einstein Condensates in Optical Lattices

Tunneling is a fascinating quantum mechanical phenomenon in which a particle passes through classically forbidden nanoscopic regions: Quantum mechanically, the particle has a finite probability of penetrating through a potential barrier even if the barrier height exceeds the kinetic energy of the particle. In 1928, G. Gamow explained the alpha decay of atomic nuclei with the quantum tunneling effect [118]. Macroscopic quantum tunneling (MQT), in which macroscopic matter waves penetrate through a potential barrier coherently, has drawn wide attention since the discovery of the Josephson effect in superconductivity [119, 120].

Macroscopic quantum tunneling has also been under keen study in the field of gaseous atomic Bose-Einstein condensates. The system is especially interesting because of the nonlinear effects due to atomic interactions, which can be controlled by tuning the interaction strength or the number of particles in the condensate. Typically, tunneling of condensates is studied in a periodic optical potential formed by a standing wave generated using lasers[14], but tunneling between two potential wells has also been investigated [122–124]. Josephson junctions have been realized with Bose-Einstein condensates in optical potentials [122–126], tunneling of condensed atoms through an accelerated optical lattice has been observed [127, 128], and the critical velocity for the onset of dissipative processes has been investigated in a periodic optical potential [129, 130]. In the experiments, the optical lattice potential is often tilted due to gravity, by applying a magnetic field or by accelerating the lattice potential. This tilted one-dimensional lattice potential is often referred to as the washboard potential, familiar from the physics of Josephson junctions, and the resulting Gross-Pitaevskii equation is often called the nonlinear Wannier-Stark problem. In Paper VII, we investigate the tunneling of a Bose-Einstein condensate through a single barrier of such a potential in the zero-temperature limit. We derive an analytical expression for the tunneling rate through the barrier, and investigate the effects of noise and harmonic drive to the tunneling rate through simulations.

[14] For a review of Bose-Einstein condensates in an optical lattice, see Ref. [121].

The derivation of the analytical formula for the tunneling rate through a potential barrier is based on three assumptions: The Thomas-Fermi parameter, *c.f.* Sec. 2.3, has to be sufficiently large such that the wave function is well approximated by the Thomas-Fermi form in the interior of the condensate. The potential barrier should be sufficiently strong, such that particle interactions can be neglected in the region of the barrier. In this approximation, the time-dependent Gross-Pitaevskii equation, Eq. (2.10), reduces to the form of the ordinary Schrödinger equation, enabling the use of a semiclassical (WKB) approximation for the order parameter in the tunneling region. Finally, the chemical potential of the condensate should not be too close to the maximum height of the potential barrier, such that the potential may be linearized to a good approximation in the vicinity of the left-hand classical turning point a, defined by $V_{\text{ext}}(a) = \mu$, see Fig. 5.1.

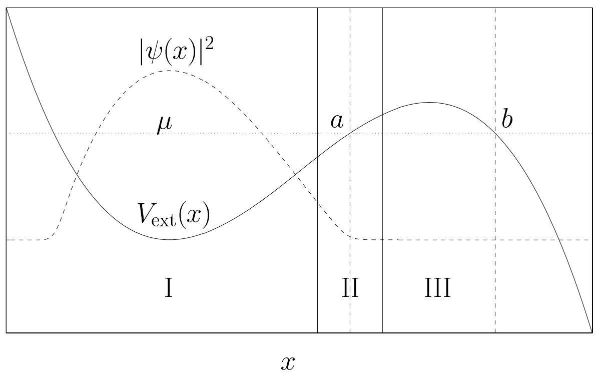

Figure 5.1: Setup for the calculation of the tunneling rate of a Bose-Einstein condensate through a potential barrier defined by $V_{\text{ext}}(x)$. The classical turning points are denoted by a and b. The wave function is assumed to be well approximated by the Thomas-Fermi form in region I, and by an Airy function in region II, the width of which has been exaggerated in the figure. In region III, the wave function is approximated by a semiclassical (WKB) form.

By linearizing the potential at $x = a$ and neglecting the nonlinear term, Eq. (2.10) reduces to the Airy differential equation. By using the Thomas-Fermi form as the left boundary condition and requiring that the order parameter vanishes for large values of the argument, the resulting unique solution provides a fair approximation in the vicinity of a. In turn, the Airy function may be extended by the semiclassical solution through the potential barrier, yielding the particle current at the right-hand turning point b. The tunneling rate through the barrier is given by

$$\Gamma \approx 0.161 \frac{\hbar}{m} \frac{F}{\tilde{g}} e^{-2W(\mu)},$$

in which $F = \partial_x V_{\text{ext}}(x)\big|_{x=a}$, $\tilde{g}$ is the effective interaction strength, and $W(\mu) = \int_a^b \sqrt{2m[\mu - V_{\text{ext}}(y)]/\hbar^2}dy$ describes the strength of the barrier for the chemical potential μ.

This result for the tunneling rate closely resembles the standard WKB result for the probability of a particle to tunnel through a potential barrier [131]: The energy of the particle is merely replaced by the chemical potential of the condensate, and the prefactor, often referred to as the attempt frequency, explicitly includes the effective interaction strength $\tilde{g}$. In order to examine the validity of the approximations, we calculated the tunneling rate also numerically for various shapes of the potential barrier and values of the interaction strength $\tilde{g}$. As expected, the approximation fails for small values of $\tilde{g}$ due to the failure of the Thomas-Fermi approximation, and for large values of $\tilde{g}$ since the chemical potential approaches the maximum of the barrier. However, Eq. (5.1) correctly predicts the tunneling rate for intermediate values of $\tilde{g}$ corresponding to several orders of magnitude in Γ.

It has been shown that the quantized energy levels in the lattice wells play an important role in the tunneling rate through a tilted periodic potential, giving rise to tunneling resonances [132–135]. Also, the effect of the optical lattice potential to the frequencies of the lowest-lying modes in magnetically trapped condensates has been investigated both theoretically [136] and experimentally [126, 137, 138]. We investigated the effect of a harmonic perturbation to the tunneling rate in our setup by adding a small term with harmonic time dependence to the strength of the optical potential. Distinct resonance peaks in the time-averaged tunneling rate were found for perturbation frequencies matching the eigenfrequencies of the dipole and the quadrupole modes. This can be interpreted as resulting from their excitation by the perturbation. In contrast to this seemingly intuitive result of enhancing the tunneling rate by perturbing the system, also suppression of the inter-well tunneling rate of a condensate in a strongly driven optical lattice has been observed [139, 140].

6 Conclusions and Discussion

Ever since the realization of the first dilute atomic Bose-Einstein condensates in 1995, remarkable progress has been achieved both in theory and experiments concerning ultracold quantum gases. Theoretical study of such systems combined with the rapidly advancing experimental techniques for measuring them provides a unique test bench for testing the validity and applicability of modern many-body quantum theories. Many fascinating phenomena have been discovered in the field during this relatively short period of research.

The research results outlined in this Thesis elucidate, in particular, the behavior of quantized vortices in dilute atomic Bose-Einstein condensates. We have studied the stability and dynamics of singly quantized vortices, vortex cluster, and multiply quantized vortices in such systems, and in addition, the tunneling of a condensate through a potential barrier. In Papers I–II, we investigated numerically the precession and displacement of off-centered vortices both in the zero-temperature limit and at finite temperatures. At ultralow temperatures, the spectrum of the off-centered vortex state is shown to contain a negative energy core-localized excitation, implying energetic instability. In Paper III, we studied numerically the dynamical stability of stationary multiply quantized vortices in different axisymmetric geometries. The states turned out to be robust against perturbations in wide regions of the parameter space. Moreover, the stability of starionary vortex clusters in non-rotating traps was studied in Paper IV. We observed that in some parameter regions, the dipole and quadrupole clusters are robust against annihilation of the structure. In Papers V–VI, we studied the dynamics of the splitting of doubly and quadruply quantized vortices, respectively. The splitting times of the multiply quantized vortices into singly quantized vortices obtained from the simulations were in fair agreement with the experimental results. The tunneling of a Bose-Einstein condensate through a single potential barrier was investigated in Paper VII, which is closely related to dynamics of condensates in optical lattice potentials. An analytical expression for the tunneling rate was derived, closely resembling the well-known formula for the probability of a single-particle tunneling event. Also, in this work we studied the effects of noise and harmonic drive to the tunneling rate.

There are still some aspects that should be taken into account in these research projects: The already published results concerning, *e.g.*, the splitting of a doubly quantized vortex under the perturbation due to the vortex creation process was calculated using a scalar condensate. The topological phase engineering technique employed in creating the vortex, however, requires a condensate consisting of three spin components. Therefore, a more accurate analysis of the initiation of the splitting process of multiply quantized vortices and further development of the system requires a multicomponent calculation. The topological phase engineering method is currently used for the creation of doubly and quadruply quantized vortices. However, recently developed methods for creating multiply quantized vortices, *e.g.*, by transferring angular momentum into a condensate with a Laguerre-Gaussian laser beam, will enable the creation of vortices with higher quantum numbers. The dynamical stability and the dynamics of the splitting of such states is yet to be investigated. Also, it should be feasible to extend the analysis concerning the tunneling of a Bose-Einstein condensate through a single potential barrier to a tilted lattice potential.

References

[1] A. Einstein, Sitzungsber. Preuss. Akad. Wiss. 261 (1924).

[2] A. Einstein, Sitzungsber. Preuss. Akad. Wiss. 3 (1925).

[3] S. N. Bose, Z. Phys. **26**, 178 (1924).

[4] H. Kamerlingh-Onnes, Comm. Phys. Lab. Univ. Leiden **122 and 124**, 1226 (1911).

[5] P. L. Kapitza, Nature **141**, 74 (1938).

[6] J. F. Allen and A. D. Misener, Nature **141**, 75 (1938).

[7] M. H. Anderson, J. R. Ensher, M. R. Matthews, C. E. Wieman, and E. A. Cornell, Science **269**, 198 (1995).

[8] K. B. Davis, M.-O. Mewes, M. R. Andrews, N. J. van Druten, D. S. Durfee, D. M. Kurn, and W. Ketterle, Phys. Rev. Lett. **75**, 3969 (1995).

[9] C. C. Bradley, C. A. Sackett, J. J. Tollett, and R. G. Hulet, Phys. Rev. Lett. **75**, 1687 (1995).

[10] J. R. Ensher, D. S. Jin, M. R. Matthews, C. E. Wieman, and E. A. Cornell, Phys. Rev. Lett. **77**, 4984 (1996).

[11] J. Söding, D. Guéry-Odelin, P. Desbiolles, F. Chevy, H. Inamori, and J. Dalibard, Appl. Phys. B **69**, 257 (1999).

[12] G. Modugno, G. Ferrari, G. Roati, R. J. Brecha, A. Simoni, and M. Inguscio, Science **294**, 1320 (2001).

[13] G. Roati, M. Zaccanti, C. D'Errico, J. Catani, M. Modugno, A. Simoni, M. Inguscio, and G. Modugno, Phys. Rev. Lett. **99**, 010403 (2007).

[14] S. L. Cornish, N. R. Claussen, J. L. Roberts, E. A. Cornell, and C. E. Wieman, Phys. Rev. Lett. **85**, 1795 (2000).

[15] T. Weber, J. Herbig, M. Mark, H.-C. Nägerl, and R. Grimm, Science **299**, 232 (2003).

[16] D. G. Fried, T. C. Killian, L. Willmann, D. Landhuis, S. C. Moss, D. Kleppner, and T. J. Greytak, Phys. Rev. Lett. **81**, 3811 (1998).

[17] A. Robert, O. Sirjean, A. Browaeys, J. Poupard, S. Nowak, D. Boiron, C. I. Westbrook, and A. Aspect, Science **292**, 461 (2001).

[18] Y. Takasu, K. Maki, K. Komori, T. Takano, K. Honda, M. Kumakura, T. Yabuzaki, and Y. Takahashi, Phys. Rev. Lett. **91**, 040404 (2003).

[19] S. Jochim, M. Bartenstein, A. Altmeyer, G. Hendl, S. Riedl, C. Chin, J. H. Denschlag, and R. Grimm, Science **302**, 2101 (2003).

[20] M. Greiner, C. A. Regal, and D. S. Jin, Nature **426**, 537 (2003).

[21] A. Griesmaier, J. Werner, S. Hensler, J. Stuhler, and T. Pfau, Phys. Rev. Lett. **94**, 160401 (2005).

[22] N. Bogoliubov, J. Phys. (Moscow) **11**, 23 (1947).

[23] L. Pitaevskii and S. Stringari, *Bose-Einstein Condensation* (Oxford University Press, New York, 2003).

[24] K. G. Singh and D. S. Rokhsar, Phys. Rev. Lett. **77**, 1667 (1996).

[25] M. Edwards, P. A. Ruprecht, K. Burnett, R. J. Dodd, and C. W. Clark, Phys. Rev. Lett. **77**, 1671 (1996).

[26] S. Stringari, Phys. Rev. Lett. **77**, 2360 (1996).

[27] D. A. W. Hutchinson, E. Zaremba, and A. Griffin, Phys. Rev. Lett. **78**, 1842 (1997).

[28] R. J. Dodd, K. Burnett, M. Edwards, and C. W. Clark, Phys. Rev. A **56**, 587 (1997).

[29] D. S. Jin, J. R. Ensher, M. R. Matthews, C. E. Wieman, and E. A. Cornell, Phys. Rev. Lett. **77**, 420 (1996).

[30] M.-O. Mewes, M. R. Andrews, N. J. van Druten, D. M. Kurn, D. S. Durfee, C. G. Townsend, and W. Ketterle, Phys. Rev. Lett. **77**, 988 (1996).

[31] D. S. Jin, M. R. Matthews, J. R. Ensher, C. E. Wieman, and E. A. Cornell, Phys. Rev. Lett. **78**, 764 (1997).

[32] D. Guéry-Odelin and S. Stringari, Phys. Rev. Lett. **83**, 4452 (1999).

[33] O. M. Maragò, S. A. Hopkins, J. Arlt, E. Hodby, G. Hechenblaikner, and C. J. Foot, Phys. Rev. Lett. **84**, 2056 (2000).

[34] O. Maragò, G. Hechenblaikner, E. Hodby, and C. Foot, Phys. Rev. Lett. **86**, 3938 (2001).

[35] G. Baym, in *Mathematical Methods in Solid State and Superfluid Theory*, edited by R. C. Clark and G. H. Derrick (Plenum Press, New York, 1968), p. 121.

[36] F. Dalfovo, S. Giorgini, L. P. Pitaevskii, and S. Stringari, Rev. Mod. Phys. **71**, 463 (1999).

[37] M. Edwards, C. W. Clark, P. Pedri, L. Pitaevskii, and S. Stringari, Phys. Rev. Lett. **88**, 070405 (2002).

[38] G. Hechenblaikner, E. Hodby, S. A. Hopkins, O. M. Maragò, and C. J. Foot, Phys. Rev. Lett. **88**, 070406 (2002).

[39] C. Raman, M. Köhl, R. Onofrio, D. S. Durfee, C. E. Kuklewicz, Z. Hadzibabic, and W. Ketterle, Phys. Rev. Lett. **83**, 2502 (1999).

[40] M. R. Matthews, B. P. Anderson, P. C. Haljan, D. S. Hall, C. E. Wieman, and E. A. Cornell, Phys. Rev. Lett. **83**, 2498 (1999).

[41] R. J. Donnelly, in *Quantized Vortices in Helium II*, edited by A. M. Goldman, P. V. E. McClintock, and M. Springford (Cambridge University Press, Cambridge, 1991).

[42] E. J. Yarmchuk, M. J. V. Gordon, and R. E. Packard, Phys. Rev. Lett. **43**, 214 (1979).

[43] M. Tinkham, in *Introduction to Superconductivity*, edited by B. Bayne and M. Gardner (McGraw-Hill, Inc., New York, 1975).

[44] G. A. Swartzlander, Jr. and C. T. Law, Phys. Rev. Lett. **69**, 2503 (1992).

[45] M. R. Andrews, M.-O. Mewes, N. J. van Druten, D. S. Durfee, D. M. Kurn, and W. Ketterle, Science **273**, 84 (1996).

[46] F. Zambelli and S. Stringari, Phys. Rev. Lett. **81**, 1754 (1998).

[47] F. Chevy, K. W. Madison, and J. Dalibard, Phys. Rev. Lett. **85**, 2223 (2000).

[48] T. Ohmi and K. Machida, J. Phys. Soc. Jpn. **67**, 1822 (1998).

[49] T.-L. Ho, Phys. Rev. Lett. **81**, 742 (1998).

[50] A. J. Leggett, Rev. Mod. Phys. **73**, 307 (2001).

[51] A. L. Fetter, Ann. Phys. **70**, 67 (1972).

[52] L. D. Landau and E. M. Lifshitz, *Mechanics* (Pergamon Press, Oxford, 1976).

[53] C. J. Pethick and H. Smith, *Bose-Einstein Condensation in Dilute Gases* (Cambridge University Press, Cambridge, 2002).

[54] S. A. Morgan, J. Phys. B: At. Mol. Opt. Phys. **33**, 3847 (2000).

[55] A. D. Jackson, G. M. Kavoulakis, and E. Lundh, Phys. Rev. A **72**, 053617 (2005).

[56] D. S. Rokhsar, Phys. Rev. Lett. **79**, 2164 (1997).

[57] A. Griffin, Phys. Rev. B **53**, 9341 (1996).

[58] S. Giorgini, Phys. Rev. A **57**, 2949 (1998).

[59] K. Burnett, in *Proceedings of the International School of Physics Enrico Fermi*, edited by M. Inguscio, S. Stringari, and C. E. Wieman (IOS Press, Amsterdam, 1999), p. 265.

[60] V. N. Popov, *Functional Integrals and Collective Excitations* (Cambridge University Press, New York, 1987).

[61] R. J. Dodd, M. Edwards, C. W. Clark, and K. Burnett, Phys. Rev. A **57**, R32 (1998).

[62] P. Nozières and D. Pines, *The Theory of Quantum Liquids Volume II* (Addison-Wesley Publishing Co., Inc., Redwood City, California, 1990).

[63] A. L. Fetter and A. A. Svidzinsky, J. Phys.: Condens. Matter **13**, R135 (2001).

[64] K. Kasamatsu, M. Tsubota, and M. Ueda, Int. J. Mod. Phys. B **19**, 1835 (2005).

[65] J. J. García-Ripoll and V. M. Pérez-Garcia, Phys. Rev. A **63**, 041603(R) (2001).

[66] J. J. García-Ripoll and V. M. Pérez-Garcia, Phys. Rev. A **64**, 053611 (2001).

[67] E. Lundh, Phys. Rev. A **65**, 043604 (2002).

[68] T. Isoshima and K. Machida, J. Phys. Soc. Jpn. **66**, 3502 (1997).

[69] A. A. Svidzinsky and A. L. Fetter, Phys. Rev. Lett. **84**, 5919 (2000).

[70] A. L. Fetter, in *Proceedings of the International School of Physics Enrico Fermi*, edited by M. Inguscio, S. Stringari, and C. E. Wieman (IOS Press, Amsterdam, 1999), p. 201.

[71] F. Dalfovo and S. Stringari, Phys. Rev. A **53**, 2477 (1996).

[72] F. Dalfovo, S. Giorgini, M. Guilleumas, L. Pitaevskii, and S. Stringari, Phys. Rev. A **56**, 3840 (1997).

[73] D. L. Feder, C. W. Clark, and B. I. Schneider, Phys. Rev. A **61**, 011601(R) (1999).

[74] B. P. Anderson, P. C. Haljan, C. E. Wieman, and E. A. Cornell, Phys. Rev. Lett. **85**, 2857 (2000).

[75] M. Guilleumas and R. Graham, Phys. Rev. A **64**, 033607 (2001).

[76] S. Giorgini, L. P. Pitaevskii, and S. Stringari, Phys. Rev. A **54**, R4633 (1996).

[77] J. Reidl, A. Csordás, R. Graham, and P. Szépfalusy, Phys. Rev. A **59**, 3816 (1999).

[78] T. Isoshima and K. Machida, Phys. Rev. A **59**, 2203 (1999).

[79] S. M. M. Virtanen, T. P. Simula, and M. M. Salomaa, Phys. Rev. Lett. **86**, 2704 (2001).

[80] M. Linn and A. L. Fetter, Phys. Rev. A **61**, 063603 (2000).

[81] E. Lundh and H. M. Nilsen, Phys. Rev. A **74**, 063620 (2006).

[82] M. Möttönen, T. Mizushima, T. Isoshima, M. M. Salomaa, and K. Machida, Phys. Rev. A **68**, 023611 (2003).

[83] H. Pu, C. K. Law, J. H. Eberly, and N. P. Bigelow, Phys. Rev. A **59**, 1533 (1999).

[84] Y. Kawaguchi and T. Ohmi, Phys. Rev. A **70**, 043610 (2004).

[85] L.-C. Crasovan, V. Vekslerchik, V. M. Pérez-García, J. P. Torres, D. Mihalache, and L. Torner, Phys. Rev. A **68**, 063609 (2003).

[86] L.-C. Crasovan, G. Molina-Terriza, J. P. Torres, L. Torner, V. M. Pérez-García, and D. Mihalache, Phys. Rev. E **66**, 036612 (2002).

[87] M. Möttönen, S. M. M. Virtanen, T. Isoshima, and M. M. Salomaa, Phys. Rev. A **71**, 033626 (2005).

[88] W. F. Vinen, Nature **181**, 1524 (1958).

[89] W. F. Vinen, Proc. Roy. Soc. (London) **260**, 218 (1961).

[90] W. Petrich, M. H. Anderson, J. R. Ensher, and E. A. Cornell, Phys. Rev. Lett. **74**, 3352 (1995).

[91] S. Inouye, S. Gupta, T. Rosenband, A. P. Chikkatur, A. Görlitz, T. L. Gustavson, A. E. Leanhardt, D. E. Pritchard, and W. Ketterle, Phys. Rev. Lett. **87**, 080402 (2001).

[92] C. Raman, J. R. Abo-Shaeer, J. M. Vogels, K. Xu, and W. Ketterle, Phys. Rev. Lett. **87**, 210402 (2001).

[93] M. F. Andersen, C. Ryu, P. Cladé, V. Natarajan, A. Vaziri, K. Helmerson, and W. D. Phillips, Phys. Rev. Lett. **97**, 170406 (2006).

[94] Z. Dutton, M. Budde, C. Slowe, and L. V. Hau, Science **293**, 663 (2001).

[95] B. P. Anderson, P. C. Haljan, C. A. Regal, D. L. Feder, L. A. Collins, C. W. Clark, and E. A. Cornell, Phys. Rev. Lett. **86**, 2926 (2001).

[96] M. Möttönen, V. Pietilä, and S. M. M. Virtanen, Phys. Rev. Lett. **99**, 250406 (2007).

[97] J. E. Williams and M. J. Holland, Nature **401**, 568 (1999).

[98] K. W. Madison, F. Chevy, W. Wohlleben, and J. Dalibard, Phys. Rev. Lett. **84**, 806 (2000).

[99] P. C. Haljan, I. Coddington, P. Engels, and E. A. Cornell, Phys. Rev. Lett. **87**, 210403 (2001).

[100] E. Hodby, G. Hechenblaikner, S. A. Hopkins, O. M. Maragò, and C. J. Foot, Phys. Rev. Lett. **88**, 010405 (2002).

[101] D. A. Butts and D. S. Rokhsar, Nature **397**, 327 (1999).

[102] E. Lundh, C. J. Pethick, and H. Smith, Phys. Rev. A **55**, 2126 (1997).

[103] J. R. Abo-Shaeer, C. Raman, J. M. Vogels, and W. Ketterle, Science **292**, 476 (2001).

[104] P. Engels, I. Coddington, P. C. Haljan, V. Schweikhard, and E. A. Cornell, Phys. Rev. Lett. **90**, 170405 (2003).

[105] A. E. Leanhardt, A. Görlitz, A. P. Chikkatur, D. Kielpinski, Y. Shin, D. E. Pritchard, and W. Ketterle, Phys. Rev. Lett. **89**, 190403 (2002).

[106] M. Nakahara, T. Isoshima, K. Machida, S.-I. Ogawa, and T. Ohmi, Physica B **284-288**, 17 (2000).

[107] T. Isoshima, M. Nakahara, T. Ohmi, and K. Machida, Phys. Rev. A **61**, 063610 (2000).

[108] S.-I. Ogawa, M. Möttönen, M. Nakahara, T. Ohmi, and H. Shimada, Phys. Rev. A **66**, 013617 (2002).

[109] M. Möttönen, N. Matsumoto, M. Nakahara, and T. Ohmi, J. Phys.: Condens. Matter **14**, 13481 (2002).

[110] L. E. Ballentine, *Quantum Mechanics: A Modern Development* (World Scientific Publishing Co. Pte. Ltd., Singapore, 1998).

[111] A. Messiah, *Quantum Mechanics Volume II, Appedix C (Section IV)* (North-Holland Publishing Company, Amsterdam, 1969).

[112] P. C. Haljan, B. P. Anderson, I. Coddington, and E. A. Cornell, Phys. Rev. Lett. **86**, 2922 (2001).

[113] P. Rosenbusch, V. Bretin, and J. Dalibard, Phys. Rev. Lett. **89**, 200403 (2002).

[114] Y. Shin, M. Saba, M. Vengalattore, T. A. Pasquini, C. Sanner, A. E. Leanhardt, M. Prentiss, D. E. Pritchard, and W. Ketterle, Phys. Rev. Lett. **93**, 160406 (2004).

[115] K. Gawryluk, M. Brewczyk, and K. Rzążewski, J. Phys. B: At. Mol. Opt. Phys. **39**, L225 (2006).

[116] A. M. Mateo and V. Delgado, Phys. Rev. Lett. **97**, 180409 (2006).

[117] M. Okano, H. Yasuda, K. Kasa, M. Kumakura, and Y. Takahashi, J. Low Temp. Phys. **148**, 447 (2007).

[118] G. Gamow, Z. Phys. **51**, 204 (1928).

[119] B. D. Josephson, Phys. Lett. **1**, 251 (1962).

[120] B. D. Josephson, Rev. Mod. Phys. **46**, 251 (1974).

[121] O. Morsch and M. Oberthaler, Rev. Mod. Phys. **78**, 179 (2006).

[122] Y. Shin, G.-B. Jo, M. Saba, T. A. Pasquini, W. Ketterle, and D. E. Pritchard, Phys. Rev. Lett. **95**, 170402 (2005).

[123] M. Albiez, R. Gati, J. Fölling, S. Hunsmann, M. Cristiani, and M. K. Oberthaler, Phys. Rev. Lett. **95**, 010402 (2005).

[124] R. Gati, B. Hemmerling, J. Fölling, M. Albiez, and M. K. Oberthaler, Phys. Rev. Lett. **96**, 130404 (2006).

[125] B. P. Anderson and M. A. Kasevich, Science **282**, 1686 (1998).

[126] F. S. Cataliotti, S. Burger, C. Fort, P. Maddaloni, F. Minardi, A. Trombettoni, A. Smerzi, and M. Inguscio, Science **293**, 843 (2001).

[127] K. W. Madison, C. F. Bharucha, P. R. Morrow, S. R. Wilkinson, Q. Niu, B. Sundaram, and M. G. Raizen, Appl. Phys. B **65**, 693 (1997).

[128] C. F. Bharucha, K. W. Madison, P. R. Morrow, S. R. Wilkinson, B. Sundaram, and M. G. Raizen, Phys. Rev. A **55**, R857 (1997).

[129] S. Burger, F. S. Cataliotti, C. Fort, F. Minardi, M. Inguscio, M. L. Chiofalo, and M. P. Tosi, Phys. Rev. Lett. **86**, 4447 (2001).

[130] F. S. Cataliotti, L. Fallani, F. Ferlaino, C. Fort, P. Maddaloni, and M. Inguscio, New. J. Phys. **5**, 71 (2003).

[131] E. Merzbacher, *Quantum Mechanics* (John Wiley & Sons, Inc., New York, 1970).

[132] S. Wimberger, R. Mannella, O. Morsch, E. Arimondo, A. R. Kolovsky, and A. Buchleitner, Phys. Rev. A **72**, 063610 (2005).

[133] S. Wimberger, P. Schlagheck, and R. Mannella, J. Phys. B: At. Mol. Opt. Phys. **39**, 729 (2006).

[134] P. Schlagheck and S. Wimberger, Appl. Phys. B **86**, 385 (2007).

[135] C. Sias, A. Zenesini, H. Lignier, S. Wimberger, D. Ciampini, O. Morsch, and E. Arimondo, Phys. Rev. Lett. **98**, 120403 (2007).

[136] M. Krämer, L. Pitaevskii, and S. Stringari, Phys. Rev. Lett. **88**, 180404 (2002).

[137] F. S. Cataliotti, L. Fallani, F. Ferlaino, C. Fort, P. Maddaloni, and M. Inguscio, J. Opt. B: Quantum Semiclass. Opt. **5**, S17 (2003).

[138] C. Fort, F. S. Cataliotti, L. Fallani, F. Ferlaino, P. Maddaloni, and M. Inguscio, Phys. Rev. Lett. **90**, 140405 (2003).

[139] H. Lignier, C. Sias, D. Ciampini, Y. Singh, A. Zenesini, O. Morsch, and E. Arimondo, Phys. Rev. Lett. **99**, 220403 (2007).

[140] C. Sias, H. Lignier, Y. P. Singh, A. Zenesini, D. Ciampini, O. Morsch, and E. Arimondo, Phys. Rev. Lett. **100**, 040404 (2008).